Reducing Aerosol Forcing Uncertainty By Combining Models with Satellite and Within-the-Atmosphere Observations: A Three-Way Street

Ralph A. Kahn[1], Elisabeth Andrews[2], Charles A. Brock[3], Mian Chin[1], Graham Feingold[3], Andrew Gettelman[4], Robert C. Levy[1], Daniel M. Murphy[3], Athanasios Nenes[5,6], Jeffrey R. Pierce[7], Thomas Popp[8], Jens Redemann[9], Andrew M. Sayer[1,10], Arlindo da Silva[1], Larisa Sogacheva[11], and Philip Stier[12]

[1] Earth Sciences Division, Goddard Space Flight Center, Greenbelt, MD USA

[2] Cooperative Institute for Research in Environmental Sciences (CIRES), University of Colorado, Boulder, Colorado and Global Monitoring Laboratory, NOAA, Boulder, CO USA

[3] Chemical Sciences Laboratory, NOAA, Boulder, CO USA

[4] National Center for Atmospheric Research, Boulder, CO USA,
Now at: Pacific Northwest National Laboratory, Richland, WA USA

[5] Laboratory of Atmospheric Processes and their Impacts, Ecole Polytechnique Fédérale de Lausanne (EPFL), Switzerland

[6] Center for the Study of Air Quality and Climate Change, Foundation for Research and Technology Hellas (FORTH), Greece

[7] Department of Atmospheric Science, Colorado State University, Fort Collins, CO USA

[8] German Aerospace Center (DLR), German Remote Sensing Data Center (DFD), Oberpfaffenhofen, Germany

[9] School of Meteorology, University of Oklahoma, Norman, OK USA

[10] University of Maryland, Baltimore County, Baltimore, MD USA

[11] Finnish Meteorological Institute, Climate Research Programme, Helsinki, Finland

[12] Department of Physics, University of Oxford, Parks Road, Oxford, UK

Corresponding author: Ralph A. Kahn (ralph.kahn@nasa.gov)

Key Points:

- Aerosol climate forcing uncertainty is virtually undiminished despite two decades of advances in many aspects of aerosol-climate science
- This review concludes that current and planned aerosol modeling, satellite and ground-based observation programs remain essential
- New, systematic aircraft aerosol particle and cloud process measurements are also needed, along with better model-measurement integration

Abstract

Aerosol forcing uncertainty represents the largest climate forcing uncertainty overall. Its magnitude has remained virtually undiminished over the past 20 years despite considerable advances in understanding most of the key contributing elements. Recent work has produced modest increases only in the confidence of the uncertainty estimate itself. This review summarizes the contributions toward reducing the uncertainty in the aerosol forcing of climate made by satellite observations, measurements taken within the atmosphere, as well as modeling and data assimilation. We adopt a more measurement-oriented perspective than most reviews of the subject in assessing the strengths and limitations of each; gaps and possible ways to fill them are considered. Currently planned programs supporting advanced, global-scale satellite and surface-based aerosol, cloud, and precursor gas observations, climate modeling, and intensive field campaigns aimed at characterizing the underlying physical and chemical processes involved, are all essential. But in addition, new efforts are needed: (1) to obtain systematic aircraft *in situ* measurements capturing the multi-variate probability distribution functions of particle optical, microphysical, and chemical properties (and associated uncertainty estimates), as well as co-variability with meteorology, for the major aerosol airmass types; (2) to conceive, develop, and implement a suborbital (aircraft plus surface-based) program aimed at systematically quantifying the cloud-scale microphysics, cloud optical properties, and cloud-related vertical velocities associated with aerosol-cloud interactions; and (3) to focus much more research on integrating the unique contributions satellite observations, suborbital measurements, and modeling, in order to reduce the uncertainty in aerosol climate forcing.

Plain Language Summary

Aerosols, such as airborne wildfire smoke, desert dust, volcanic and pollution particles, affect Earth's climate by reflecting (some also absorb) sunlight. These aerosol particles also play key roles in cloud formation and evolution, further affecting the planet's energy balance. The magnitudes of these effects, and even the underlying mechanisms, represent the largest uncertainty in climate modeling. Despite two decades of advances in many aspects of aerosol-climate science, aerosol climate forcing uncertainty is virtually undiminished. Yet, reducing this uncertainty is critical for any effort to attribute, mitigate, or predict climate changes. We adopt a

measurement-oriented perspective to assess the strengths and limitations of measurement and modeling programs, and conclude that current and planned efforts need to continue. However, in addition, new efforts are needed: (1) to obtain aircraft *in situ* measurements that capture systematically aerosol particle properties for the major aerosol airmass types, globally, (2) to conceive, develop, and implement an aircraft and surface-based program aimed at filling gaps in our understanding of the interactions between aerosol particles and clouds, along with (3) focusing much more research on integrating the unique contributions of satellite observations, suborbital measurements, and modeling, to reduce the uncertainty in our understanding of Earth's changing climate.

1 Introduction

The confidence with which Earth's present and possible future climate can be simulated depends upon our ability to represent the factors that heat and cool the system, and the processes that mediate the environmental response. In this context, radiative forcing describes the energy fluxes that drive the climate system. Changes in the radiative forcing of climate are caused primarily by perturbations of atmospheric constituents, mainly greenhouse trace gases (GHGs), airborne particles (aerosol particles), and clouds. By convention, positive forcing produces net surface heating, whereas negative forcing produces cooling. Understanding changes in the radiative forcing of climate is critical for any effort to attribute, mitigate, or predict climate change.

Although GHGs contribute most of the positive radiative forcing, its magnitude is tightly constrained, so uncertainty in the climate forcing by aerosol particles dominates the uncertainty in forcing changes overall (e.g., Forster et al., 2021; Watson-Parris & Smith, 2022). Globally, aerosol forcing is generally negative. As one illustration of the importance of reducing aerosol forcing uncertainty, decreases in aerosol amount in some regions can lead to increased surface heating (Jenkins et al., 2022; Quaas et al., 2022). Thus, understanding the factors driving climate change, and improving our ability to predict climate changes under different future scenarios, requires a reduction in the uncertainty in aerosol climate forcing. This includes both the direct

radiative forcing due to light scattering and absorption by airborne particles, as well as indirect effects due to the interactions between aerosol particles and clouds (ACI).

There are fundamental reasons why aerosol radiative forcing is more difficult to quantify than forcing from GHGs. First, present-day aerosol forcing is often assessed relative to assumed pre-industrial conditions, which are presumed to be largely unaffected by human influences (e.g., IPCC, 2013). Yet, there are few observational constraints on the pre-industrial aerosol state (e.g., Carslaw et al., 2017). For example, for aerosol amount there is no analog to the ice core data that defines pre-industrial GHG concentrations, and unlike gases, aerosol microphysical properties vary greatly. Further, even for the present day, the distinction between natural and anthropogenic aerosol is often ambiguous. Is wind-blown dust to be considered natural or anthropogenic when it is emitted in regions experiencing desertification due to increased use of water resources, over-grazing and other farming practices, or some combination of larger-scale environmental changes of uncertain natural or anthropogenic origin? The same question applies to smoke aerosol from lightning-ignited wildfires that might be greatly intensified by anthropogenically enhanced warming, drying, or forest management practices. Also, in practical terms, remote-sensing data alone cannot be interpreted precisely enough in most cases even to distinguish natural aerosol from aerosol that are unambiguously anthropogenic when directly sampled (see Section 2 below). These issues with historical data and the attribution of today's emissions contribute to large uncertainty in the difference between aerosol forcing under both pristine and present-day conditions (Carslaw et al., 2013; Hamilton et al., 2018).

Note that the total direct radiative forcing by aerosol includes natural sources, representing the dominant contribution to the global atmospheric aerosol mass load, plus anthropogenic aerosol. The Intergovernmental Panel on Climate Change (IPCC) calls the total quantity the aerosol direct radiative effect, and refers to the anthropogenic component as the aerosol direct forcing. Given the ambiguities from an observational perspective, we use the term "aerosol forcing" to include anthropogenic and natural direct and indirect forcings and adjustments; we specify direct or indirect where needed.

A second reasons why aerosol radiative forcing is more difficult to quantify: aerosol particles are vastly more spatially and temporally heterogeneous than GHGs, due to relatively short

atmospheric lifetime, sources that are highly non-uniform in space and time, and particle physical and chemical evolution that varies with atmospheric conditions. As such, frequent, global observation of aerosol distribution and key properties must be provided to capture this heterogeneity. Not only is aerosol amount highly variable at different locations and times, aerosol light scattering, light absorption, and cloud nucleating properties vary considerably with source, composition, and particle evolution. As we discuss in Section 2, these factors cannot be determined adequately from remote sensing alone.

Finally, aerosol particles produce relatively large adjustments to forcing compared to GHGs. That is, aerosol particles have secondary climate impacts, such as changing the atmospheric stability profile or altering cloud radiative properties, lifetime, and precipitation. These semi-direct (ambient heating by light-absorbing particles), indirect (e.g., increased particle concentration causing additional cloud droplet or ice crystal formation), and other effects represent aerosol-induced changes in the atmosphere that can cause changes in surface temperature indirectly. For example, vertical redistribution of aerosol extinction can alter the atmospheric thermodynamic structure, and atmospheric adjustments can even change the sign of black carbon forcing in the upper atmosphere compared to the surface (e.g., Lau et al., 2008; Samset et al., 2013), whereas for major GHGs such as CO_2, adjustments are estimated to represent much smaller fractional contributions (Forster et al., 2021). A combination of measurements and modeling is required to constrain adjusted forcing.

Reducing the magnitude of aerosol forcing uncertainty to a value comparable to that of CO_2 and other long-lived GHGs (estimated at ± 0.35 W/m^2 and ± 0.23 W/m^2, respectively; IPCC, 2013) will require greater observational constraints than near-future satellite measurements alone are likely to provide. A lower bound on the uncertainty range of just the direct component of the total global-mean all-sky aerosol forcing (i.e., that due to scattering and absorption by airborne particles but not their indirect effects on clouds) is estimated as ±1.1 W/m^2 when considering anticipated data from a planned next-generation NASA satellite mission aimed at addressing global climate change issues (1σ; Thorsen et al., 2021). (This number represents 30% or more of the global all-sky aerosol forcing by most estimates.) Systematically incorporating prior information beyond that available from current or near-future large-scale observations is necessary to reduce uncertainties in the role aerosol particles play in climate forcing. Thorsen et

al. (2021) suggest that incorporating additional particle property constraints might approximately halve the direct forcing uncertainty estimate, though the even larger uncertainty associated with the indirect effects of aerosol particles on clouds is more difficult to reduce or even to estimate. Thus, to reduce climate modeling uncertainties, there is a crucial need for better particle optical, microphysical, and chemical property information than can be provided by satellite measurements alone. This persistent uncertainty is reflected in part by the enormously diverse, yet often simplistic, particle property assumptions made in different models (e.g., CCSP, 2009). Such diversity is also true of the aerosol optical model priors (i.e., initial guesses) or climatologies adopted as constraints in leading satellite aerosol retrieval algorithms (e.g., Remer et al., 2005; Levy et al., 2007; Kahn & Gaitley, 2015; Kim et al., 2018; Holzer-Popp et al., 2013). Further, the uncertainties in aerosol-cloud interactions must be reduced as well.

Previous reviews of aerosol climate forcing tend to adopt a model-centric perspective, appropriately, as models offer the ability to make climate predictions. Such reviews can provide formal estimates of aerosol forcing and its uncertainties based on current modeling, often also taking account of the limited constraints provided by available measurements (e.g., Bellouin et al., 2020). Here we take a more measurement-focused perspective, reviewing where we stand at present on the contributions measurements can make and their relationships with models, allowing us to also identify gaps that need to be filled.

Figure 1 provides a framework for discussing research activities aimed at reducing uncertainty in aerosol forcing, and also helps organize the material presented in subsequent sections. It illustrates the unique and essential roles played by satellite observations, measurements made within the atmosphere (often termed "suborbital" measurements when taking a perspective that includes global satellite measurements), as well as aerosol and climate modeling, in closing the gap in aerosol forcing uncertainty relative to that of GHGs. The arrows and associated, color-coded annotations in Figure 1 highlight the required *exchange of information* between these three elements. (The common expression "a two-way street" means A affects B, but B also affects A. Here, A affects B and C, B affects A and C, and C affects A and B; hence, a three-way street.) From the synthesis provided by this review, we conclude that satellite measurement and modeling efforts and plans for addressing aerosol climate forcing are relatively mature. However, the uncertainty in aerosol impacts on climate directly, and indirectly through their

interactions with clouds, could be significantly reduced through specific enhancements to the suborbital component, along with greater synergy among the three elements. As such, we review the satellite and modeling contributions first (Sections 2 and 3, below), then consider the suborbital element in Section 4, and provide a synthesis in Section 5 and the Conclusions. The view presented here is informed in part by discussions in the AeroCom and AeroSat communities over the past decade (https://aerocom.met.no and https://aero-sat.org, respectively; last accessed: March 2023), the work of the Systematic Aircraft Measurements to Characterize Aerosol Air Masses (SAM-CAAM) Science Definition Team (Kahn et al., 2017), and the collective insights of the authors of the current paper.

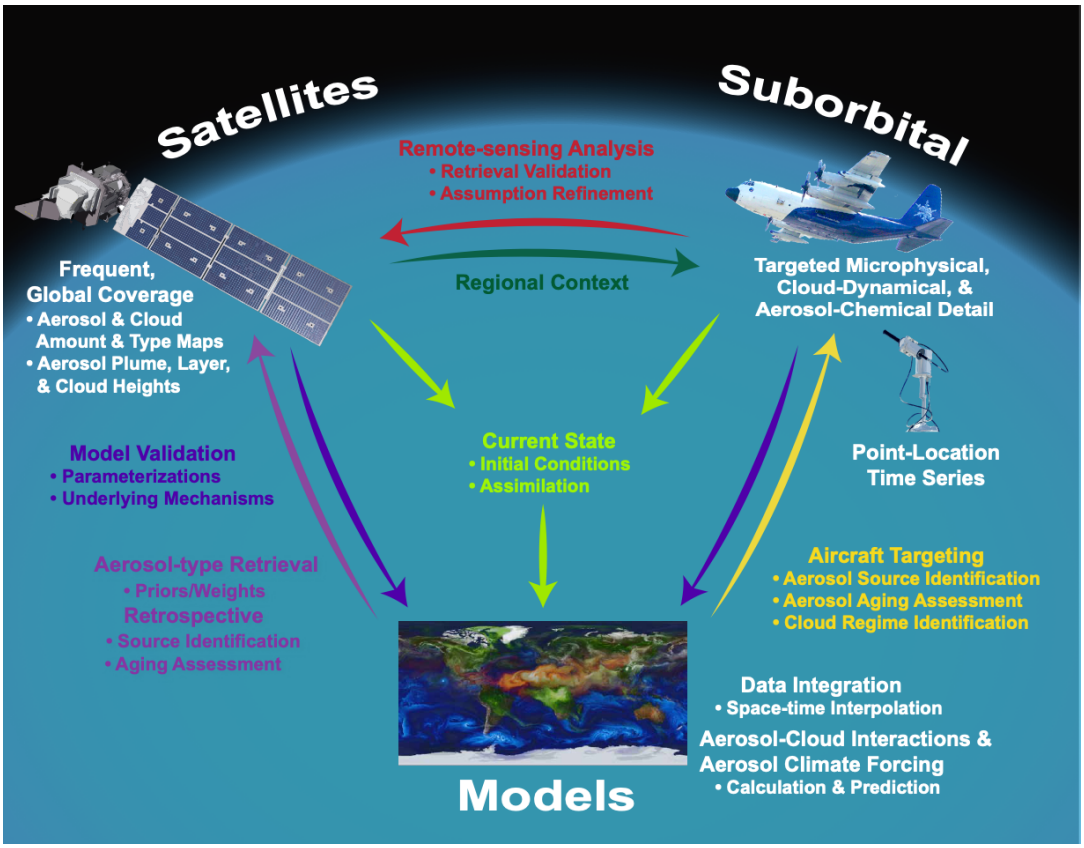

Figure 1. A framework for considering the research activities needed to reduce the persistent aerosol forcing uncertainty. It illustrates the relationships among the measurements, the modeling contributions, and the interactions among these elements that we identify as central to

194 this effort (adapted from Kahn, 2012). The arrows and associated, color-coded annotations
195 indicate the contributions each element can make to the other two – a three-way street.

196

197 **2. Satellite Contributions**

198 Earth-orbiting satellites offer the opportunity to collect frequent, global data, and are well suited
199 to remotely measure quantities that vary on kilometer or even smaller spatial scales, at daily or
200 even shorter timescales.

201 **2.1. Aerosol Amount – Total-Column Optical Depth and 3-D Distribution**

202 For more than 20 years, satellites have demonstrated the ability to provide extensive spatial and
203 frequent temporal coverage of aerosol column amount globally, primarily under clear-sky
204 conditions, and generally reported as the mid-visible aerosol optical depth (AOD). This quantity
205 is widely used as a constraint on climate models, or for model evaluation (e.g., Kinne et al.,
206 2006; Buchard et al., 2017; Gelaro et al., 2017; Randles et al., 2017; Rubin et al., 2017;
207 Schutgens, et al., 2020; Gliß et al., 2021), though non-negligible differences among AOD
208 retrieval products must yet be addressed (Sogacheva et al., 2020; Li et al., 2020). Tables
209 summarizing currently available satellite AOD products are given in Sogacheva et al. (2020) and
210 Kahn and Samset (2022). Space-based lidars provide the altitudes of extended aerosol layers
211 with the precision of tens of meters (e.g., Winker et al., 2009; Yorks et al., 2016), and usually
212 sample well downwind of aerosol sources, where the AOD tends to be low enough for the signal
213 to penetrate the column under cloud-free conditions. Lidar measurements are complemented by
214 near-source aerosol plume height from multi-angle imagery obtained in low-Earth or
215 geostationary orbit (Kahn et al., 2008; Nelson et al., 2013; Carr et al., 2022). Such information
216 can help characterize aerosol vertical extent or source injection height in models (e.g., van
217 Donkelaar et al., 2010; Val Martin et al., 2018). Although coverage by these measurements is
218 currently limited, their precision has demonstrated value in constraining and/or validating models
219 aimed at simulating downwind wildfire smoke and volcanic ash dispersion (e.g., Zhu et al.,
220 2018a; Vernon et al., 2018). A number of satellite-based, passive-imager spectral techniques, at
221 wavelengths ranging from the ultraviolet (UV) to the infrared, offer greater aerosol layer-height

222 coverage, at the cost of additional assumptions that increase uncertainty (e.g., Jeong & Hsu,
223 2008, Griffin et al., 2020; Go et al., 2020; Kylling et al., 2018; Lu et al., 2021; Lyapustin et al.,
224 2020). Passive-imager techniques, especially in UV channels, have also been effective in
225 constraining aerosol occurrence, and even amount, over cloudy scenes (e.g., Torres et al., 2012;
226 Meyer et al., 2015; Sayer et al., 2019).

227 Models require the source strength in addition to the injection height to represent aerosol
228 sources. Efforts at using satellite AOD measurements to constrain source strength have applied
229 either inverse modeling to infer source location along with strength from broad-swath-imager
230 AOD maps (e.g., Dubovik et al., 2008), or forward modeling, where a measured smoke-plume
231 AOD snapshot is compared to a model, run in the forward direction and initialized with varying
232 source strengths (Petrenko et al., 2017). These methods work best for high-AOD aerosol plumes
233 with little background or aged aerosol in the scene to complicate interpretation. Other
234 approaches, specifically for wildfires, use the magnitude of the 4-micron brightness temperature
235 anomaly, which can be observed from remote sensing, combined with empirically derived,
236 ecosystem-specific emission factors, to estimate smoke source strength (e.g., Ichoku & Ellison,
237 2014; Wiggins et al., 2020; see review by Andreae, 2019). Next-generation spacecraft
238 deployments promise to greatly increase coverage frequency and diurnal sampling, with
239 instrumentation such as multi-angle, multi-spectral polarimeter imagers and High Spectral
240 Resolution Lidars offering advanced measurement capabilities (e.g., https://aos.gsfc.nasa.gov,
241 last accessed, June 2022). Further, recent advances in estimating satellite-retrieved AOD
242 uncertainty, even at the individual pixel level, have increased the utility of the satellite AOD
243 measurements as constraints on aerosol forcing (Sayer et al., 2020; Witek et al., 2018).

244 The largest remaining uncertainties in the measured global distribution of aerosol amount for
245 climate forcing applications are due to (a) difficulties in retrieving AOD over snow, ice, bright or
246 topographically complex land, and cloud-covered surfaces, (b) accounting in satellite retrieval
247 algorithms for the detailed aerosol light-scattering and light-absorption properties, as well as the
248 hydration state of different aerosol types under ambient conditions that affect retrieved aerosol
249 amount, (c) obtaining adequate spatial coverage for aerosol layer-height observations, and (d)
250 specifying the relative-humidity-dependent Mass Extinction Efficiency (MEE) that is required to
251 translate between AOD derived optically from remote sensing and the dry aerosol mass that is

bookkept in climate and air quality models. Nighttime AOD is also poorly sampled by passive sensors including broad-swath imagers at present, and it can be important in accounting for the infrared part of the energy balance, especially in areas where airborne mineral dust is abundant. This is probably a secondary issue in representing global aerosol climate forcing, given the uncertainties under daylight conditions (e.g., Adebiyi & Kok, 2020); however, some space-based thermal IR (Vandenbussche et al., 2013; Capelle et al., 2018) and even visible (Wang et al., 2016) remote-sensing techniques hold promise to provide extensive nighttime AOD coverage beyond what is possible with active sensors. As discussed in subsequent sections, appropriate combinations of modeling and suborbital measurements with the satellite observations (Figure 1) appear to be key to addressing the limitations of the space-based AOD data record.

2.2. Satellite Constraints on Aerosol Particle Properties

Satellite observations have up to now been less successful at providing the quantitative particle optical, microphysical, and chemical properties needed to model aerosol forcing. For example, uncertainty in aerosol light-absorption, usually represented by the spectral single-scattering albedo (SSA), is comparable or possibly of greater importance compared to AOD in setting the overall uncertainty in aerosol direct forcing of Earth's energy budget (McComiskey et al., 2008; Loeb & Su, 2010; Thorsen et al., 2021; Li et al., 2022). Along with aerosol vertical distribution, SSA is also critical for modeling the semi-direct aerosol effect, i.e., the aerosol impact on solar-energy absorption and atmospheric heating, along with the attendant effects on clouds.

The ability to obtain quantitative or even qualitative constraints on properties such as particle size, SSA, and sphericity depends on retrieval conditions as well as instrument characteristics. These variables can be derived from multi-angle, multi-spectral observations when the surface is not too complex and the AOD is sufficiently high – typically exceeding 0.2 to 0.5 at mid-visible wavelengths. This is often challenging, as the global average mid-visible AOD is ~0.14 (e.g., Andrews et al., 2017). For example, much of wildfire smoke instantaneous radiative forcing occurs over extended areas downwind, where smoke AOD < 0.1 (Schill et al., 2020). In addition, the sun-spacecraft observing geometry must provide an adequate range of scattering angles for

279 robust results using this technique (e.g., Kalashnikova et al., 2013; Kahn & Gaitley, 2015;
280 Fougnie et al., 2020).

281 Temporal compositing of single-view sensor measurements acquired at different times with
282 different viewing angles (Lyapustin et al., 2021) and/or different AOD (e.g. Seidel and Popp,
283 2012; Wells et al., 2012) can also be used to enhance their information content and obtain tighter
284 AOD or SSA constraints. Polarized, multi-spectral multi-angular measurements improve
285 retrieval sensitivity to the real part of the particle refractive index and to the width of the particle
286 size distribution, as well as broadening the range of conditions under which meaningful particle-
287 type constraints can be obtained (e.g., Mishchenko & Travis, 1997; Dubovik et al., 2011;
288 Hasekamp et al., 2011). Despite this, systematic differences in aerosol absorption derived from
289 different algorithms applied to the same polarimetric sensor still exceed the requirements for
290 adequate constraints on aerosol forcing (Schutgens et al., 2021). Although the deployment of
291 new polarimeters with increased polarimetric accuracy (e.g., Werdell et al., 2019) should reduce
292 these discrepancies to some degree, algorithmic assumptions will still be required (e.g., when
293 layers containing different aerosol types occur in the atmospheric column); as with all new
294 measurements, the quality of the results remains to be demonstrated.

295 Space-based, two-channel backscatter lidar with polarization sensitivity currently provides a
296 height-resolved classification of six empirically defined aerosol types operationally, using the
297 retrieved depolarization ratio, attenuated backscatter, layer top and base altitudes, and surface
298 type as input (Kim et al., 2018). Future spacecraft deployment of High-Spectral-Resolution Lidar
299 (HSRL) instruments promises to refine lidar aerosol-type retrieval by constraining, in addition,
300 the light extinction-to-backscatter ratio (e.g., Burton et al., 2012; Hélière et al., 2012; Russell et
301 al., 2014; Dawson et al., 2017), a key aerosol-type-dependent microphysical property that must
302 be assumed when interpreting backscatter-only observations in terms of aerosol amount. The
303 inclusion of an ultraviolet channel in a future space-based lidar instrument for greater particle-
304 type discrimination, especially with depolarization sensitivity, is also possible (Burton et al.,
305 2015; Nicolae et al., 2018; Papagiannopoulos et al., 2018).

306 Overall, within the AOD and other retrieval caveats discussed above, satellite remote sensing can
307 contribute to constraining direct aerosol forcing by mapping aerosol types qualitatively and

identifying differences in particle size and light-absorption. However, to date, constraints from satellites alone on SSA and particle size distribution lack the coverage, the accuracy, as well as the error characterization, required for closing the aerosol forcing uncertainty gap in most environments.

When retrieval conditions are favorable, some general deductions about the mechanisms driving aerosol property evolution have also been gleaned from satellite data, such as near-source in wildfire smoke and volcanic plumes. For example, changes in AOD, and in retrieved effective particle size and light-absorption downwind of major sources, have been used to infer size-selective or size-independent particle deposition, particle hydration or oxidation, secondary aerosol formation, the condensation of volatiles on existing particles, and particle activation processes (Junghenn Noyes et al., 2020; Flower & Kahn, 2020a; b). In addition, having plume-level wind vectors, e.g., derived from multi-angle stereo imaging, makes it possible to estimate timescales for the observed transitions, at least near major aerosol sources. Coincident field data, primarily from aircraft making detailed *in situ* measurements and in some cases from ground observers, have been essential for building confidence in these inferences made from remote-sensing observations (e.g., Junghenn Noyes et al., 2020). At the same time, extensive, qualitative aerosol property mapping from satellites can place the detailed aircraft measurements, acquired, e.g., along disjoint transects of a smoke plume, into the larger context of plume-particle evolution. This complementary exchange of information is illustrated in Figure 1 (red and dark green arrows). Further, despite the qualitative nature of satellite-based particle-evolution-process deductions, the satellite data also offer broad spatial coverage that allows for multi-year assessment of the dominant particle evolution processes and associated timescales where data quality is adequate (e.g., Junghenn Noyes et al., 2022).

Several approaches have been taken to using satellite measurements and the associated inferences as validation or constraints on models (Figure 1, blue and light green arrows). In addition to statistical comparisons between aggregated satellite observations and models of particle evolution processes and timescales, by configuring models to simulate specific instrument measurements, more quantitative, direct comparisons between models and observations can be made in some cases. The results can be especially useful as a means of diagnosing model behavior, leading to better constraints on model parameterizations, at least

338 statistically. Such work has been performed mainly on daily snapshots from polar-orbiting
339 instruments. However, as the capabilities of instruments on geostationary (Gupta et al., 2019;
340 Lim et al., 2018; Zhang et al., 2020a) and even more remote platforms (Marshak et al., 2018)
341 advance, data from these sources promise to increase constraints on aerosol processes by
342 resolving the time-evolution of particle properties over large areas.

343 **2.3. Strengths and Limitations of Space-based Aerosol-Cloud Interactions (ACI)**
344 **Observations**

345 From the satellite perspective, reducing the forcing uncertainties due to the indirect effects of
346 aerosol particles on clouds is yet more challenging, given the subtlety and complexity of the
347 aerosol as well as the cloud processes involved, and the range of spatial and temporal scales on
348 which they operate (e.g., reviews by Rosenfeld et al., 2014 Seinfeld et al., 2016; Mülmenstädt &
349 Feingold 2018; McCoy et al., 2016; Quaas et al., 2020; Bellouin et al., 2020). Cloud-formation
350 processes require aerosol particles to serve as cloud condensation nuclei (CCN), except under
351 very cold, homogeneous-nucleation conditions. More generally, the CCN size spectrum and
352 concentration, particle hygroscopicity, and SSA are all required to model cloud-droplet
353 formation and ACI. However, the mutual interactions between aerosol particles and clouds mean
354 that the challenge is much greater than just measuring CCN, because a host of other cloud
355 microphysical and dynamical processes change ('adjust'), depending in part on CCN properties
356 and concentrations.

357 A fundamental limit to the contribution satellites can make regarding ACI is that particles
358 smaller than about 0.1 μm in diameter are difficult to characterize with remote sensing; they are
359 very inefficient at scattering light and are essentially indistinguishable from the background
360 atmospheric gas. Yet, such small particles can represent a significant fraction of the activated
361 CCN, particularly under high updraft velocities (e.g., Twomey, 1974; Stier, 2016). Broad-swath,
362 single-view imagers can provide AOD and can constrain its spectral dependence under good
363 retrieval conditions. The extinction Ångström Exponent (ANG), defined as the negative slope of
364 AOD vs. wavelength (both in log space) is inversely proportional to particle size, provided a
365 single aerosol mode dominates the atmospheric column. The product of AOD and ANG (derived
366 from AOD retrieved at several wavelengths), designated the aerosol index (AI), yields a metric

that weights AOD toward smaller (CCN-like) sizes (Nakajima et al., 2001). As an estimate of CCN, AI is a qualitative indicator at best, in part because particle hygroscopicity is generally unconstrained by remote-sensing measurements but can dominate the relationship between retrieved AOD and particle number, especially for small particles (Kapustin et al., 2006; Cao et al., 2023), and in part because extrapolating the observed part of the aerosol spectrum to smaller sizes engenders additional assumptions. However, AI is often treated as quantitative for lack of other observational constraints.

At the other end of the CCN size distribution, giant CCN, on the order of several microns in diameter, can have an inordinately large effect on precipitation formation in warm clouds, even at concentrations on the order 1/liter (Feingold et al., 1999), far too low to be retrieved from space-based remote sensing. High concentrations of coarse-mode and giant CCN (~ 1-2 microns in diameter and larger) can also have a disproportionately large impact on cloud supersaturation and susceptibility to aerosol perturbations (e.g., Ghan et al., 1998; Morales Betancourt & Nenes, 2014). As such, giant CCN characterization must rely primarily on suborbital measurement. Some recent advances in aircraft instrumentation and analysis are improving our ability to characterize giant CCN *in situ* (e.g., Jung et al., 2015; Dadashazar et al., 2017; Gonzalez et al., 2022). Yet, giant nuclei measurement remains challenging, due to issues such as losses in conventional inlets (e.g., Wilson et al., 2004), sizing uncertainties in wing-mounted probes (e.g., Gonzalez et al., 2022), generally low number concentrations, and the need to know the time-history of relative humidity exposure to relate dry and ambient particle properties.

Particle light-absorption is also challenging to constrain quantitatively with remote sensing (Section 2.2 above). Yet aerosol composition, particularly smoke or dust aerosol having low SSA, can play an important role in driving cloud-mediated radiative forcing. Such particles can heat the atmosphere, reducing the ambient relative humidity and causing cloud-droplet evaporation (the so-called semi-direct effect). Further, by affecting the atmospheric vertical stratification, they can either suppress (e.g., Koren et al., 2004) or possibly enhance convection, depending on the location of the aerosol (Koren et al., 2005; Jiang & Feingold, 2006). Well-

394 defined smoke plumes can apparently also alter mesoscale (Lee et al., 2014) and large-scale
395 (Williams et al., 2022) circulation patterns.

396 Satellite-based mapping of aerosol amount over extended regions is obtained from passive
397 measurements of column-integrated AOD. Attempts at correlating AOD directly with CCN
398 concentration measured *in situ* have yielded only qualitative relationships (e.g., Andreae, 2009;
399 Shinozuka et al., 2015; Shen et al., 2019), and vertical decoupling introduces significant
400 additional uncertainty (Stier, 2016). Of particular relevance for this application, the CCN that
401 actually participate in the cloud-droplet-formation process are typically just below cloud base, a
402 region inaccessible to passive measurements from space. These CCN can be measured directly
403 only with *in situ* aircraft instruments or inferred from surface remote sensing, by inverting cloud
404 microphysical measurements (Feingold et al., 1998), athough indirect methods offer promise for
405 some situations (e.g., Rosenfeld et al., 2016).

406 Further complicating the satellite contribution to measuring ACI is the complexity of interpreting
407 remote-sensing observations in the vicinity of clouds (e.g., Marshak et al., 2021). This region,
408 sometimes termed the "twilight zone," contains a continuum of hydrated aerosol, evaporating
409 cloud droplets, and cloud fragments (Koren et al., 2007). To interpret remote-sensing
410 observations, both "cloud contamination" of the aerosol signal and light-scattering by the cloud
411 must be taken into account. Standard retrieval algorithms assume 1-D radiative transfer whereas
412 these situations are inherently three-dimensional; the 3-D radiative transfer that applies here can
413 produce significantly different AOD retrieval results and aerosol forcing estimates (e.g., Wen et
414 al., 2007; Yang et al. 2022). Furthermore, considering the hygroscopic growth of particles in the
415 vicinity of clouds as a continuum means that the aerosol forcing is driven by the 3-D spatial
416 distribution of humidity in the cloud field (which varies on much smaller scales than the aerosol
417 properties (e.g., Anderson et al., 2003)).

418 Atmospheric dynamics plays an important role in determining the effects of aerosol on clouds,
419 and this too is difficult to constrain from space at the relevant spatial and temporal scales, and
420 with the required accuracy. Water vapor supersaturation, responsible for cloud droplet and ice
421 crystal formation, is generated by expansion cooling that is directly proportional to vertical
422 velocity. The fraction of particles that activate to form cloud droplets is often strongly dependent
423 on updraft velocity, although aerosol number concentration, size distribution, and to a lesser

extent composition also affect the result (Feingold, 2003; Ervens et al., 2005; McFiggans et al., 2006). Vertical velocity is more important when cloud supersaturation is low; such "velocity-limited conditions" occur frequently around the globe (Reutter et al., 2009; Morales Betancourt & Nenes, 2014; Sullivan et al., 2016). When low supersaturation occurs under high aerosol (polluted) conditions, drop concentration depends on both CCN concentration and vertical velocity (e.g., Kacarab et al., 2020; Bougiatioti et al., 2020; Georgakaki et al., 2021**;** Foskinis et al., 2022); however, factors such as aerosol size distribution and chemical composition can also become more important under these conditions (e.g., Rissman et al., 2004; McFiggans et al., 2006). In aerosol-poor environments such as the Arctic, the factor limiting droplet formation is often the number concentration of CCN, and vertical velocity uncertainty becomes less important (e.g., Feingold et al., 2003; McFiggans et al., 2006). Yet, vertical velocity is rarely constrained by measurements contemporaneous with aerosol amount and properties such as particle size distribution and hygroscopicity (e.g., Kacarab et al. 2020; Bougiatioti et al. 2020). Further, despite its high spatial variability globally (order 10s of meters), vertical velocity only can be measured at the required accuracy and spatial resolution with limited sampling, using active Doppler lidar or Doppler radar from suborbital platforms (e.g., Guimond et al., 2014; Schroeder et al., 2020). At least until next-generation satellite instruments are developed, updraft velocity measurements relevant to drop and ice formation are unlikely to be possible from spacecraft alone.

The most widely observed ACI process is cloud brightening, which is caused by an increase in CCN concentration generating an increase in cloud droplet number, and all else being equal, a decrease in droplet size (Twomey, 1974). However, this conceptually simple mechanism is also strongly affected by cloud adjustments (e.g., Twomey, 1977; Quaas et al., 2020). Much work has focused on aerosol-related cloud brightening with all other factors, especially cloud liquid water path (LWP), held constant. However, both LWP and cloud fraction have been shown to exhibit non-monotonic responses to aerosol perturbations. Under clean conditions, increases in aerosol tend to increase LWP, whereas under polluted conditions LWP might be reduced (Wang et al. 2003; Ackerman et al. 2004, Bretherton et al. 2007; Gryspeerdt et al. 2019). Similar results appear to be valid for cloud fraction (e.g., Xue et al. 2008; Gryspeerdt et al. 2022). Although some in-cloud processes can be inferred from satellite observations (e.g., Rosenfeld et al., 2016), at least with assumptions that must be carefully assessed (Grosvenor et al., 2018; Zhu et al.,

2018b), the spatial and temporal resolution required to observe most ACI processes is beyond present-day satellite-measurement capabilities. Further, the lack of simultaneous, detailed, space-based observations of the multiple factors of import in these processes precludes resolving the key subtleties in these aspects of ACI with satellite data alone.

The processes associated with cloud brightening are relatively fast, e.g., on order 10 minutes for aerosol activation in shallow clouds to approximately 20 h for LWP and cloud fraction adjustments (Glassmeier et al., 2021). However, aerosol particles can also alter regional-scale circulation patterns on much longer timescales, which in turn change cloud amount (e.g., Menon et al., 2002). From climate-forcing and even extreme-weather perspectives, these circulation responses are of great importance (Soden & Chung, 2017; Persad et al., 2022; Williams et al., 2022). This is one aspect of ACI where satellite observations play a dominant role, providing frequent, regional-to-global-scale measurements of cloud amount and bulk cloud properties (Figure 1).

In summary, many of the factors that dominate aerosol-cloud-radiation interactions, such as CCN concentration, particle size and composition, are difficult to measure with space-based remote sensing; this is especially true for efforts to obtain coincident aerosol and related cloud properties. As such, knowledge of these quantities remains limited on a global scale (e.g., Seinfeld et al., 2016), leaving model-simulated aerosol indirect effects inadequately constrained by observations. Except in special circumstances and with stringent assumptions (e.g., Pahlow et al., 2006; Rosenfeld et al., 2016; Dawson et al., 2020), quantitative constraints on nearly all the key variables needed to characterize detailed ACI are beyond the capabilities of existing and currently planned space-based remote-sensing instruments. Nevertheless, satellite observations of well-defined aerosol sources such as ship tracks, industrial point sources of pollution, wildfire smoke and volcanic plumes, represent “natural laboratories” that have proven particularly useful in studying ACI, because the unaffected surroundings provide a control for the confounding factors associated with meteorology, at least to first order (Christensen et al., 2022). Also, the large datasets obtained from space can support fine-scale stratification of meteorological

conditions, allowing the aerosol effects on clouds to be isolated statistically in some cases (e.g., Zamora & Kahn, 2020).

Characterizing ACI globally requires knowledge of co-varying aerosol properties and vertical velocity from suborbital platforms, as a function of meteorological variables that can also be monitored over broad regions from space or derived from reanalysis. The suborbital measurements would be targeted at characterizing statistically the key variables at cloud scale for a range of specific cloud types and meteorological conditions, some of which could be retrieved from space-based instruments with enough specificity to map out the appropriate ACI regimes. Steps in this direction have been taken by several field campaigns, including VOCALS (Bretherton et al., 2010; Mechoso et al., 2014), ORACLES (Redemann et al., 2021), and recently ACTIVATE (Sorooshian et al., 2019; 2021). The complexity of ACI and resulting ramification calls for a further, comprehensive program of targeted efforts of this kind, especially with simultaneous radiative flux measurements included, so the indirect effect can be quantified and radiative closure assessed. Specifying such a program is beyond the scope of the current review.

3. Regional-to-Global-Scale Modeling Contributions

Climate modeling is of course essential for calculating direct and indirect aerosol forcing globally, for filling gaps in the observational record, and for making climate forcing and response predictions based on assumed future emissions scenarios. Such models can also play a key role in targeting aircraft *in situ* measurements to sample specific aerosol and cloud situations, and subsequently, in identifying the aerosol sources and aging histories for aerosol airmasses captured by satellite and suborbital observations (Figure 1, purple and yellow arrows,

504 respectively). However, from emissions to aerosol climate forcing, models incorporate large
505 numbers of assumptions and parameterizations of complex physical and chemical processes.

506

507 **3.1. Model Representation of Aerosol Particle Properties**

508 There are a few fundamental steps models take in simulating the global distribution of aerosol
509 particles, and then calculating aerosol direct radiative forcing (e.g., Kinne et al., 2003). First,
510 aerosol paticles and their precursor emissions are usually prescribed from existing datasets, such
511 as for combustion aerosol (e.g., van der Werf et al., 2017), or calculated interactively by the
512 models, typically for sea salt (de Leeuw et al., 2011) and mineral dust (e.g., Zender et al., 2003;
513 Pu et al., 2020) based upon meteorological conditions such as near-surface wind shear and
514 surface properties. The emission inventories specify the initial state of aerosol mass, and might
515 provide some indication of particle composition, size distribution, and aerosol precursor gases
516 (e.g., Randerson et al., 2012; Hoesly et al., 2018). These data, as well as the source locations and
517 vertical distribution of emissions, must be supplied to the model, based on measurements where
518 available (see Section 2), and inferred or assumed elsewhere. Then the atmospheric aerosol
519 concentrations are calculated from simulated atmospheric processes, including chemical and
520 physical transformation, transport, dry deposition, and wet removal. These processes are
521 typically represented as parameterizations of physical mechanisms or as empirical relationships
522 that depend on aerosol physical and chemical properties; they can be coupled interactively to
523 meteorological conditions from the host general circulation model. Next, the aerosol optical
524 properties, including the wavelength-dependent extinction (scattering + absorption), SSA, and
525 particle single-scattering phase function (or asymmetry factor) are calculated as a function of
526 aerosol mass composition, particle size distribution, particle-type-specific hygroscopic growth,
527 refractive indices, and sometimes particle shape, limited by the extent to which these properties
528 have been measured for the aerosol types involved (see Section 4 below). In bulk aerosol
529 treatments, the microphysical properties are prescribed, although a growing number of modal
530 and sectional aerosol models calculate them explicitly from microphysical schemes (e.g., Stier et
531 al., 2005; Liu et al., 2007; Bauer et al., 2008; Mann et al., 2010; Kokkola et al., 2018). The
532 resulting optical and microphysical properties vary greatly depending on model

parameterizations, choice of parameter values, and assumed meteorological conditions. Finally, the direct aerosol radiative effects are derived from the calculated or assumed aerosol optical properties, simulated mass loading, and meteorological conditions, typically using fast, simplified radiative transfer models, though often traceable to more detailed models (e.g., Iacono et al., 2008).

The best-constrained aerosol-related quantity in this process is probably the mid-visible AOD, thanks to the modern-era satellite observations from multiple space-borne platforms (see Section 2 above). This provides a basis for models to adjust their parameterizations and assumptions to better match at least the AOD. Soon after monthly global satellite AOD data products became available, they were used to validate model results (e.g., Kinne et al., 2006; Gliß et al., 2021). More recently, satellite as well as surface-network-based AOD has been used to constrain some models directly. Assimilation of aerosol data has become routine in many operational and research forecasting organizations (e.g., Benedetti et al., 2009; Randles et al., 2017). The International Cooperative for Aerosol Prediction (ICAP) offers a multi-model ensemble that includes major aerosol forecasting activities from around the world, often assimilating satellite-derived AOD as a constraint (Xian et al., 2019).

However, reproducing the global, mid-visible AOD to within the satellite retrieval uncertainty, typically a few tenths under good retrieval conditions, does not resolve the fundamental issues created by the intermediate steps leading up to the AOD calculation. This is clearly demonstrated in AeroCom studies showing that the diversity of model-simulated total AOD is much smaller than the diversities of individual aerosol species and other key quantities such as mass loading, mass extinction efficiency, and lifetime, for which there are far fewer observational constraints (Kinne et al., 2006; CCSP, 2009; Gliß et al., 2021). Apparently, different models match the observed AOD for different reasons. Further, within models, the diversity of all aerosol-forcing-related quantities increases on regional spatial and seasonal/sub-seasonal temporal scales in most cases.

Although mid-visible AOD is by far the most common observable assimilated in these models, assimilation of lidar extinction and/or backscatter profiles as well as multi-wavelength reflectances from passive sensors is being explored (e.g., Benedetti et al., 2009; Sekiyama et al.,

2010; Zhang et al., 2011; 2020b). Generally, in aerosol data assimilation, aerosol optical properties are specified by the host model; measurements are used to adjust only the aerosol constituent mass concentrations. As such, the process is limited by uncertainties in both the measurements and the model parameterizations. Further, the simultaneous adjustment of optical properties, particle size, and mass concentration has not yet received adequate attention, especially given the increasing availability of hyperspectral data (e.g., Lee et al., 2015).

3.2. Application of Model Aerosol Type to Complement Measurements

Aerosol composition based on source characteristics, transport, removal processes, as well as microphysical and chemical evolution, can be extracted from model simulations and used to complement satellite measurements. Specifically, models can in principle provide priors to aerosol remote-sensing retrieval algorithms, or retrospective refinement to the aerosol-type mixing state as part of the satellite aerosol-retrieval process when the aerosol-type information content of the satellite-observed signals is limited (Figure 1, purple arrow). For example, the model-simulated aerosol species, advected downwind, can be used to weight a loosely constrained range of particle properties derived from the satellite observations; the model-simulated aerosol type depends only on the source-receptor relationship, whereas the specificity of satellite-retrieved aerosol-type constraints varies with retrieval conditions, and is greatly diminished when the AOD is low or when a dominant type is lacking (Section 2 above). The challenge is associating the aerosol properties assumed by the model with the aerosol types derived by the satellite retrieval algorithm. An early effort keyed on ANG and absorbing AOD to connect aerosol properties simulated by an aerosol transport model with the satellite-retrieved aerosol type (Li et al., 2015). To make the comparisons, AOD fractions of the modeled aerosol components were ranked, reducing dependence of the result on absolute AOD values. This application is in its infancy, and the process of associating satellite-constrained aerosol types with aerosol as represented in models requires substantial further investigation.

However, there is also considerable uncertainty in model-simulated particle property detail, arising in part from the lack of such detail in emission inventories used to initialize climate models, and limitations in the representation of particle microphysical and chemical aging processes. Model representation of aerosol properties often fails to capture the complexity found

591 in nature, particularly in bulk models lacking microphysics, and generally, differences among
592 commonly used aerosol representations in models can produce very different aerosol forcing
593 results in model simulations (Nazarenkpo et al., 2017). Further, it has been shown many times in
594 the literature that large diversity exists in model-simulated aerosol properties and both direct and
595 indirect radiative forcing (e.g., Shindell et al., 2013; Schutgens et al., 2013; Stier et al., 2013;
596 Fiedler et al., 2019). The first comprehensive inter-model comparisons of the main parameters
597 determining the aerosol radiative forcing were documented by the AeroCom community, with
598 simulation results from more than a dozen global models (Textor et al., 2006, 2007; Kinne et al.,
599 2006; Schulz et al., 2006). Since then, the diversity among model simulations of aerosol forcing
600 and climate response has persisted, especially at regional scales (e.g., Koch et al., 2009; Huneeus
601 et al., 2011; Samset et al., 2014; Tsigaridis et al., 2014; Pan et al., 2015; Kim et al., 2014, 2019;
602 Bian et al., 2017; Sand et al., 2017; Mortier et al., 2020; Gliß et al., 2021; Lee et al., 2021)
603 despite the advances in satellite observation and *in situ* measurement (summarized in Sections 2
604 and 4, respectively).

605 For climate modeling applications, aerosol amount is quite well measured by the combination of
606 satellite and ground-based instruments (Section 2.1 above), which also places constraints on
607 aerosol source strength (e.g., Dubovik et al., 2008; Petrenko et al., 2017), transport, and to some
608 extent, removal (e.g., Das et al., 2017; Kim et al., 2014; 2019; Reid et al., 2009). However,
609 aerosol-type diversity and the associated uncertainty in aerosol-species-specific physical and
610 optical properties, especially SSA (e.g., McComiskey et al., 2008; Loeb & Su, 2010; Thorsen et
611 al., 2021), continue to play a leading role in simulated aerosol direct forcing uncertainty. The
612 availability of generally good, global AOD datasets from satellite remote sensing (Section 2
613 above) helps constrain transport and removal processes in models, although uncertaintities in
614 other, aerosol-type-specific properties such as SSA and mass extinction efficiency lead to much
615 poorer constraints on mass loading and direct aerosol forcing. For indirect forcing, uncertainty
616 due to limited observational constraints on the processes by which aerosol particles affect
617 different cloud types (Section 2.3 above) combines with particle and cloud property uncertainties
618 (Carslaw et al., 2013). In addition, vertical velocity at cloud-scale cannot be resolved in current
619 climate models, yet, uncertainties in this quantity can make models overly sensitive to aerosol or
620 meteorological conditions, obscuring the underlying sources of modeled indirect forcing
621 uncertainty (Sullivan et al., 2016). In addition, only a few models treat the aerosol effects on ice

622 nucleation for cold clouds (e.g. Gettelman et al 2012), further contributing to spread due to
623 model diversity. These aerosol-climate-forcing issues in turn make major contributions to the
624 diversity in model climate prediction, and *model diversity represents only a lower bound on*
625 *model uncertainty, especially when model diversity is reduced as a consequence of model inter-*
626 *comparison studies rather than based on comparisons with measurements*. *To obtain estimates*
627 *of actual model uncertainty requires having appropriate measurements againt which to*
628 *compare*.

629 **3.3. Strengths and Limitations of the Aerosol-Forcing Modeling Process**

630 ***Within models, the terms associated with aerosol climate forcing can be isolated.*** Aerosol
631 radiative forcing is usually defined as the change of net irradiance (in W m^{-2}) at either the
632 tropopause after stratospheric temperature adjustment (e.g., Ramaswamy et al., 2001), or at the
633 top-of-atmosphere, provided stratospheric adjustment has little effect on the aerosol radiative
634 forcing (e.g., Schulz et al., 2006). As such, aerosol radiative forcing (ARF) is the combined
635 result of aerosol-radiation interactions (ARI) and ACI (Boucher et al., 2013). ARI represents the
636 change aerosol particles make to the incoming solar radiation reaching Earth's surface through
637 both direct and semi-direct effects. As discussed in Section 2.3, ACI accounts for the impact
638 aerosol particles have on cloud albedo and lifetime when they serve as CCN (or Ice Nuclei, IN),
639 in turn altering radiative fluxes. ARF can produce positive or negative net climate forcing,
640 depending on the aerosol type, meteorological conditions, surface properties, and the spatial
641 distribution of aerosol particles relative to clouds.

642 To calculate ARI, models must represent the vertically and spectrally resolved aerosol extinction,
643 SSA, and phase function (or asymmetry factor) of airborne particles. As discussed in Sections
644 3.1 and 3.2 above, these quantities depend on the emissions inventories and meteorology used to
645 initialize the model, the atmospheric transport, removal, chemical processes used to simulate
646 aerosol mass concentrations and composition, and the underlying aerosol physical and optical
647 properties including particle mixing state, size distribution and shape, hydroscopic growth, and
648 spectral-dependent complex refractive indices. The parameterizations associated with each step
649 in model simulation entail considerable uncertainties. Although most of the required quantities
650 are either inferred from measurements or derived from theory, measurements to constrain the

models are grossly limited or unavailable. Extrapolating sparse optical property measurements over much larger spatial and temporal domains is risky, resulting in large uncertainties propagating throughout the multiple stages of radiative forcing calculations (e.g., Schutgens et al., 2013).

Modeling the ACI component of aerosol radiative forcing is even more uncertain than that for ARI, as it involves the liquid and ice cloud formation processes, lifetime, and properties along with aerosol particle microphysical characteristics (Section 2.3 above; comprehensively reviewed by Bellouin et al., 2020). For example, changes in CCN can affect cloud-droplet number; clouds can respond with 'adjusted' mass and extent. Similarly, aerosol particles can affect precipitation and latent heat release, although changes in precipitation on regional scales are mediated primarily by energy and water budget considerations (e.g., Held & Soden, 2006; O'Gorman et al., 2012; Gettelman & Sherwood, 2016; Dagan and Stier, 2020). Studies of aerosol impacts on deep convective clouds find that with increased aerosol loading, precipitation and convective updrafts might increase, decrease, or remain relatively unchanged, apparently depending upon other, unidentified factors (Tao et al., 2012; Boucher et al., 2013), results that entail significant model uncertainties (Marinescu et al., 2021). As discussed earlier, quantifying aerosol indirect effects also involves modeling cloud formation, lifetime, and properties, and is highly sensitive to cloud-scale vertical velocities and the above-mentioned aerosol characteristics. Many of the relevant processes operate on spatial scales far smaller than the resolution of global models and are therefore either highly parameterized or simply not included, such as some aerosol effects on convective clouds. Large Eddy Simulations (LES) are valuable research tools, complementary to climate models in that they can resolve many of the smaller-scale processes; however, they still entail assumptions that are often unconstrained by measurements, are impractical to run over large areas or long time periods, and cannot provide estimates of forcing (e.g., Bellouin et al., 2020).

Further, the review of aerosol forcing modeling above addresses only present-day conditions. In most modeling-oriented climate assessments such as the IPCC reports, aerosol radiative forcing requires accounting for the difference between present-day and "pre-industrial" conditions, i.e.,

679 conditions at a time when it is assumed anthropogenic influences were minimal, commonly taken
680 as 1750 or 1850. This of course engenders furthur uncertainties, as discussed in Section 1.

681

682 **4. The Role of Aircraft and Ground-based *In situ* and Remote-sensing Measurements**

683 Existing aircraft and ground-based *in situ* and remote-sensing aerosol measurements are
684 sometimes described collectively as the suborbital aerosol program-of-record. These data
685 provide the key information that has been applied by both the satellite and modeling
686 communities as constraints on aerosol microphysical properties (e.g., Reddington et al., 2017;
687 Gliß et al., 2021) and vertical structure (Watson-Parris et al, 2019). The particle property
688 measurements are used to assign priors and to make other assumptions in many satellite remote-
689 sensing aerosol retrieval algorithms. They also form the basis for the microphysical property
690 assumptions of aerosol source characteristics in most models, and they can contribute to model
691 validation (Figure 1). For climate applications, these suborbital measurements are usually used in
692 a statistical sense due to their significant spatial and/or temporal sampling limitations.

693 **4.1. Surface-based Observation Network and Aircraft Field Campaign Contributions**

694 Networks of surface-based remote-sensing instruments, such as sun photometers (e.g., the
695 Aerosol Robotic Network, AERONET, Holben et al., 1998; the Marine Aerosol Network,
696 MAN, Smirnov et al., 2011) and aerosol lidars (e.g., the Micro-Pulse Lidar Network, MPLNET,
697 Welton et al., 2001; the European Aerosol Research Lidar Network, EARLINET, Pappalardo et
698 al., 2014), generate a substantial database of aerosol amount, vertical distribution, and some
699 particle property information. In addition, heavily instrumented surface sites, such as the US
700 Department of Energy's Atmospheric Radiation Measurement (ARM) program at their Southern
701 Great Plains site and Mobile Facilities (e.g., Vogelman et al. 2012; Mather & Voyles, 2013)
702 contribute detailed, local aerosol, cloud, and radiation measurements. (A table of leading surface-
703 based aerosol measurement networks is given in Kahn et al. (2004).) Direct *in situ* sampling at
704 ground stations can add physical, optical, and chemical detail to the remotely sensed particle
705 optical properties and can document long-term variability, but such measurements are acquired
706 only near or at the surface and at only a few sampling sites, mostly concentrated in a few regions

of the globe (e.g., The US Interagency Monitoring of Protected Visual Environments network, IMPROVE, Malm & Hand, 2007; the Surface Particulate Matter Network, SPARTAN, Snider et al., 2015; the Global Atmospheric Watch (GAW) network, Andrews et al., 2019; Rose et al., 2021; Laj et al., 2020; the European Commission's Aerosol, Clouds, and Trace Gases Research Infrastructure (ACTRIS) (https://www.actris.eu; last accessed: March 2023); plus studies of collected data by Fanourgakis et al., 2019; Burgos et al., 2020).

Intensive aircraft field campaigns complement the surface-based measurements, offering much greater flexibility in sampling the atmosphere near and downwind of aerosol sources; this allows for *in situ* as well as remote-sensing measurement of transported aerosol layers aloft as they evolve, and further, can provide insight into the processes involved in aerosol evolution and aerosol-cloud interaction (e.g., the Atmospheric Tomography Mission, ATom, Brock et al., 2021; the Studies of Emissions and Atmospheric Composition, Clouds and Climate Coupling by Regional Surveys campaign, SEAC^{4}RS, Toon et al., 2016; The Green Ocean Amazon Experiment, GOAMAZON, Martin et al., 2017; the Observations of Aerosols above Clouds and their Interactions campaign, ORACLES, Redemann et al., 2021; the Aerosol Cloud Meteorology Interactions over the Western Atlantic Experiment, ACTIVATE, Sorooshian et al., 2021). However, such campaigns can target only selected regions and are usually limited in time, typically lasting only a few weeks or months. Finally, laboratory analysis of collected samples is sometimes required to obtain compositional and some key optical results, but are currently also severely limited in scope (e.g., Di Biagio et al., 2017; McNeill et al., 2020).

4.2. Strengths and Limitations of Aerosol Property Data Available from Suborbital Sources

Aerosol property databases have been developed in the past. A leading example is the Optical Properties of Aerosols and Clouds (OPAC) database (Hess et al., 1998). It provides tabulated, digital, microphysical and optical properties, covering UV, visible, and infrared spectral ranges, for aerosol components as well as mixtures representing various aerosol types, and includes data calculated at a number of relative humidity values. The need for such databases is demonstrated by the widespread use of OPAC optical properties in models, satellite remote sensing retrieval algorithms, and as precomputed packages for use in radiative transfer codes (e.g., Chin et al., 2002; Thomas et al., 2009; Dee et al., 2011; Gasteiger & Wiegner, 2018; Vicent et al., 2020).

Indeed, OPAC has over 3,000 citations at the time of writing, according to Google Scholar. However, OPAC has known, significant limitations, due to the lack of representative (or in some cases, any) measurements of the required aerosol properties. These limitations have been documented in the literature (e.g., Colarco et al., 2013; Zieger et al., 2013; Alvarado et al., 2016) and, despite the availability of much better instrumentation than that used decades ago to help construct OPAC, this situation persists today.

As consistently and systematically measured particle chemical, microphysical, and optical properties are currently lacking, it is difficult to critically assess and improve model assumptions. Recent efforts to collect retrospective, *in situ* aerosol data into a better organized "program-of-record" promise to help refine our sense for the range of particle property values in different places (e.g., Reddington et al., 2017; Balkanski et al., 2021; Schuster & Trepte, 2021). However, past aerosol property measurements were not designed to provide the comprehensive inputs needed for global climate modeling. To be most useful as constraints on modeling aerosol forcing, suborbital measurements of particle microphysical and chemical properties must meet the following four criteria:

• A ***statistical sampling*** of key variables for major aerosol airmass types is needed. (An aerosol airmass describes the spatial and temporal distribution of aerosol particles having similar properties, based on remote-sensing retrieval of aerosol type or on model simulation from a particular source and evolution.) Aircraft *in situ* aerosol measurements are not often made with the aim of obtaining the distribution (e.g., the probability distribution function or PDF) of particle property values associated with specific aerosol types. Except at sparse surface-based sampling stations, a limited number of individual measurements of a given aerosol airmass type is the best we currently have in most cases, whereas to establish the PDF of a quantity, a sufficient number of measurements is required so that subsequent measurements reproduce the distribution of values already obtained.

• A ***suite of specific physical, chemical, and optical quantities*** is needed to adequately characterize an aerosol type for climate applications, and would also be useful for air quality modeling (Table 1). All the required types of measurements have been made in the past, but

764 rarely have they all been made together for the same aerosol airmass and under appropriate
765 ranges of meteorological conditions.

766 • ***Particle property evolution during transport needs to be characterized***. The properties of
767 many aerosol types change significantly as they age. As such, the particle properties of major
768 aerosol types need to be characterized systematically *downwind from the source* (or upwind
769 toward the source) to adequately capture the aging process. Further, the *source, the age, and the*
770 *associated environmental conditions* need to be recorded for each sample, best done in most
771 cases by aerosol transport modeling (Figure 1, yellow arrow). (The timescales for particle
772 evolution vary. Changes in wildfire smoke particles and secondary aerosol formation typically
773 occur over minutes to hours (e.g., Yokelson et al., 2009; Kleinman et al., 2020), whereas
774 alteration of mineral dust properties can take days (e.g., Denjean et al., 2016) and is unlikely to
775 be fully captured during a single aircraft flight.) Such aircraft measurements can also acquire
776 information characterizing *aerosol variability at spatial scales of a few km or less*, which can be
777 important for representing sub-grid-scale aerosol properties and ACI processes in climate models
778 (Haywood et al., 1997; Fast et al., 2022). With the help of aerosol transport modeling and/or
779 synoptic-scale satellite observations, aerosol sources and transport history can be determined,
780 even when aerosol layers are superposed at different elevations and from different sources, but
781 again, this has not been done for much of the program-of-record.

782 • ***Uncertainty characterization is critical*** to assess the resulting uncertainty in derived aerosol
783 forcing. However, estimates of measurement uncertainty are difficult to obtain for many aircraft
784 *in situ* instruments. This situation can be improved considerably with techniques that were
785 unavailable for most field campaigns until recently. For example, open-path instruments, some
786 existing and some in development, can measure aerosol properties under ambient conditions.
787 Such properties include aerosol scattering and extinction, as well as particle size distribution
788 (Martins, 2016) and light-absorption estimates (Gordon et al., 2015). These measurements
789 facilitate uncertainty estimate calculations for the particle hygroscopicity derived from other, in-
790 aircraft measurements. In addition, the open-path instruments can produce uncertainty estimates

(or even corrections) for directly measured inlet efficiency, which is especially important for super-micron particles.

Table 1*. The suite of aerosol properties that need to be measured systematically, primarily from aircraft, and the purpose of each, for the climate-forcing application[†].

Aerosol Properties Obtained from *In Situ* Measurements[§] and Integrated Analysis	
Spectral extinction coefficient	- To constrain and to interpret spectral Aerosol Optical Depth (AOD)
Spectral absorption or single-scattering albedo	- To determine atmospheric spectral light-absorption and heating - To constrain spectral AOD retrievals
Particle hygroscopic growth factor	- To connect particle properties with ambient RH conditions - To model particle activation and aerosol-cloud interactions
Particle size distribution	- To model particle optical properties and loss mechanisms - To model particle activation and aerosol-cloud interactions - As a complement to chemical composition discrimination - Required for deriving aerosol Mass Extinction Efficiency (MEE)
Particle composition	- For source identification - To classify measurements in terms of aerosol types as specified in most models, e.g., sea salt, sulfate, mineral dust, black carbon (BC), brown carbon (BrC), especially important for aerosol-cloud-interaction modeling - To support deriving properties of the anthropogenic fraction, as needed to calculate anthropogenic aerosol "climate" forcing (also supports air quality applications)
Spectral single-scattering phase matrix [all possible angles]	- To calculate radiation fields - To constrain multi-angle radiance AOD retrievals - *Polarized* – to help determine aerosol type, and to constrain remote-sensing observations where polarized data are included
Mass extinction efficiency (MEE)	- To translate between optical remote-sensing measurements and model aerosol mass [Can be derived from integrated analysis of particle size distribution and extinction coefficient, with density deduced from particle compositional constraints or measured directly from samples]
Real Refractive Index	- To model aerosol optical properties

	- To constrain AOD retrievals to the level-of-detail required for aerosol forcing
Variables Providing Meteorological Context	
Carbon Monoxide (CO; also possibly CO_2, NO_2, O_3)	- As a tracer for smoke, to help distinguish smoke from urban pollution in some cases - For modeling heterogeneous reactions, secondary aerosol formation
Ambient temperature, Pressure, and Relative humidity (RH)	- To help interpret ambient measurements - To translate between instrument and ambient conditions
Aircraft 3-D location	- To relate aircraft measurements to model simulations and to any available satellite observations, for source identification and aging history
Variables Providing Ambient, Remote-Sensing Context	
Ambient Spectral single-scattering phase matrix [all possible angles]	- To assess in-aircraft measurements by comparing with ambient conditions - To help calculate radiation fields and constrain remote-sensing AOD retrievals - *Polarized* – to help determine aerosol type, and to constrain remote-sensing retrievals where polarized data are included
Ambient Spectral extinction coefficient	- To constrain remote-sensing spectral AOD retrievals and assess in-aircraft measurements by comparing with ambient conditions
Large particle / cloud probe	- To provide information about dust and other particles larger than the inlet size cut of other instruments - As an independent measure of possible cloud impact on the reliability of other data
Aerosol layer heights	- To determine flight levels for subsequent direct sampling - To correlate with meteorological conditions - As a constraint on trajectory modeling to identify aerosol sources and evolution

797

798 *Adapted from Kahn et al., 2017; © American Meteorological Society. Used with permission.
799 This table was originally developed for aircraft aerosol measurements, as these can sample
800 aerosol aloft and can characterize particle property evolution systematically. However, a subset
801 of these measurements acquired from surface-based instruments can contribute as well,
802 especially for the near-surface components that are difficult to sample from airborne platforms.
803 †The variables in this table are aimed at characterizing aerosol properties for the major aerosol
804 air mass types in general. CCN and Ice Nucleii (IN) would be included, especially in the
805 hygroscopic growth factor and size distribution measurements. However, systematic and
806 comprehensive measurements of additional cloud and meteorological variables associated with

aerosol-cloud interactions, for the major cloud types and meteorological regimes, globally, as introduced in Section 2.3, would require a different aircraft program, beyond the scope of this review.

§These quantities are typically measured inside the aircraft, at low or at least altered RH.

Although many current models are not equipped to apply detailed *in situ* aerosol property measurements directly due to the simplicity of their parameterizations, such information remains critical for characterizing model error. By systematically collocating measured and modeled aerosol optical properties in space and time, the probability distribution of errors in these parameters can be estimated. Such diagnostics can help refine model parameterizations and better quantify the uncertainties in the derived aerosol radiative forcing, especially those associated with simplified assumptions and parameterizations. And as computer capabilities allow climate models to advance, the applicability of information provided by such measurement detail will increase. For example, more sophisticated parameterizations of aerosol-cloud interactions and more subtle particle physical and chemical changes during particle aging could be captured in the simulations.

5. Discussion – Addressing Suborbital Data Limitations

Of the three elements shown in Figure 1, the suborbital measurement component is the least well addressed for the aerosol climate forcing application by existing and planned efforts. In this section, we review the more comprehensively defined possibilities for aerosol property measurements first, and touch on those for ACI subsequently.

The current aerosol measurement program-of-record does not meet the criteria summarized in Section 4. This is reflected in the *diversity of assumed aerosol properties* in remote-sensing retrieval algorithms, and the even greater particle property diversity among model assumptions (e.g., CCSP, 2009; Myhre et al., 2013; Gliß et al., 2021). The lack of consensus about aerosol intensive properties provides some indication of what is yet to be achieved with systematic *in situ* aerosol measurements. *All measurements have uncertainties. However, in situ measurements*

835 *can provide the most direct way to quantify particle SSA and size distribution, offer by far the*
836 *best constraints on particle hygroscopicity and the CCN size spectrum, and produce the only*
837 *available constraints on MEE and actual particle composition.* This is illustrated, for example,
838 by the work of Brock et al. (2021).

839 As such, a comprehensive database of key *in situ* measurements targeting the major aerosol
840 airmasses would fill this persistent gap in our ability to model the effects of aerosol particles on
841 climate. It would also add value to several decades of existing as well as all future global satellite
842 remote-sensing measurements by providing more robust, complete, and detailed particle
843 microphysical property information than is currently available to use as priors or constraints on
844 remote-sensing retrieval algorithms. For data assimilation, such measurements would provide a
845 better basis for quantifying errors arising from faulty or uncertain assumptions about aerosol
846 optical properties in the retrieval process and would open the door for the assimilation of aerosol
847 properties beyond AOD. The data would be of value for air quality applications as well, by
848 contributing to the accuracy of aerosol species as represented in air quality models.

849 One simplifying factor for developing a database addressing current needs is that, *for a given*
850 *source in a given season, the particle intensive microphysical and optical properties tend to be*
851 *repeatable*, even as the aerosol amount varies on many spatial and temporal scales. For example,
852 although the amount of dust raised from a particular desert source region can vary diurnally,
853 seasonally, and interannually, the emitted dust microphysical properties generally remain
854 unchanged (e.g., Reid et al., 2008). Similarly, wildfires consuming the same vegetation types in
855 the same ecosystem and season tend to produce smoke particles having similar properties (e.g.,
856 Reid et al., 2005; Junghenn Noyes et al., 2022). This means a program aimed at making the suite
857 of key *in situ* particle intensive property measurements systematically is at least feasible.

858 Complementary satellite measurements are also needed (Figure 1), frequently, over large spatial
859 scales for regional context, (a) to map the varying extensive properties, i.e., aerosol amounts and
860 3-D spatial distributions of different aerosol types, and (b) to limit as much as possible sampling
861 bias (e.g., Schutgens et al., 2017). Aerosol type, the classification possible based on particle
862 size, shape, and SSA constraints that can be derived from satellite remote-sensing measurements,
863 is the key to linking the extensive aerosol air masses, mapped out frequently and globally by

satellites, with the detailed intensive properties that can only be derived from *in situ* measurements. Hence, systematic *in situ* aircraft measurements will have made a key contribution to reducing aerosol forcing uncertainty once they have adequately characterized the detailed particle microphysical properties for major aerosol sources and their downwind evolution. Further, the *in situ* measurements can be acquired under non-precipitating cloudy conditions, in some cases even if the aerosol particles are concentrated within a cloud layer, and the observations need not be obtained in synchrony with satellite observations (although doing so at times would be important, e.g., for remote-sensing retrieval validation and assessment of consistency among different measurement approaches).

Aircraft *in situ* programs aimed at measuring aerosol microphysical or optical properties systematically have been deployed in the past, though with different objectives from the one discussed here (e.g., the Civil Aircraft for Regular Investigation of the Atmosphere Based on an Instrument Container, CARIBIC, Nguyen et al., 2006; the Vertical Profiles of Aerosol Optical Properties over rural Oklahoma program, Andrews et al., 2011; the Vertical Profiles of Aerosol Optical Properties over Central Illinois program, Sheridan et al., 2012). Some recent airborne science projects have also included components aimed at characterizing aerosol properties or processes systematically (Brock et al., 2021; Redemann et al., 2021, Sorooshian et al., 2019; 2021). These efforts offer some guidance as to how such programs might operate. However, the level of effort needed to characterize statistically the required suite of aerosol properties (Table 1), for many aerosol types, has been beyond the scope of past campaigns, which have either focused on one specific region or included only commercial airline pathways, and some quantities such as MEE have not been constrained in most of these experiments.

A possible future aircraft program addressing the needed aerosol microphysical properties for reducing aerosol forcing uncertainty has been outlined previously, showing that the key variables could be measured with a relatively small but dedicated aircraft, and with technologies that existed even in 2014, though there have been some significant improvements in instrumentation since (Kahn et al., 2017). The aircraft would fly two-to-three times per week from an initial base of operations, with fixed flight plans aimed at sampling all the major, climatologically likely aerosol airmasses accessible from the base, as identified in advance from model simulations and satellite aerosol-type mapping. The flight plan would begin with a high-altitude traverse along

894 one of the pre-determined paths, and a simple lidar on board would determine the elevations of
895 the aerosol layers below. The layers would then be sampled, as far up- or downwind as feasible,
896 and the aircraft would return to base.

897 Once the PDFs of the key variables were acquired for the accessible aerosol airmasses, the
898 aircraft would move to a new base of operations, again informed by an analysis of aerosol
899 transport model simulations and aircraft siting considerations. Unlike typical aircraft field
900 campaigns, the data would be processed routinely, probably at a central location, as is common
901 for NASA satellite missions. In addition to helping deployment planning in advance, by
902 identifying important source locations and likely dispersion pathways as sampling targets,
903 aerosol transport models would also be run routinely during deployment, to characterize the
904 sources and aging histories of the aerosol particles sampled during each flight (Figure 1, yellow
905 arrow). As opportunities arose, the aircraft would overfly ground stations for cross-validation,
906 and could also participate in intensive field campaigns when appropriate. Taking account of
907 typical aircraft maintenance considerations, the availability of basing facilities, and the
908 seasonality of some aerosol sources, we estimate that a deployment of roughly three-to-four
909 years would be required to sample the major aerosol airmasses of North America. There is
910 additional uncertainty in this estimate, however, due to limited knowledge about the number of
911 samples required to obtain PDFs for different key variables and for different aerosol types,
912 depending also on the capabilities of the designated aircraft and the robustness of the
913 instrumentation. The successful demonstration of such a program could engender similar
914 programs hosted in other regions around the world, leading to characterization of the major
915 aerosol airmass types, globally.

916 The requirements for suborbital measurements to comprehensively reduce uncertainties in
917 modeling ACI processes and effects are not as well established as those described above for
918 addressing aerosol properties. A suborbital ACI measurement program could be considerably
919 more complex. Reviews of past modeling and measurement work (e.g., Rosenfeld et al., 2014;
920 Mülmenstädt & Feingold, 2018; Bellouin et al., 2020) and experience from recent aircraft
921 campaigns aimed at characterizing aerosol particles, clouds, and their interactions in specific
922 regions (Behrenfeld et al., 2019; Sorooshian et al., 2019; 2021; Crosbie et al., 2022) provide
923 some indication of what would be involved. Both aerosol and cloud properties would need to be

924 measured for this application, on spatial scales ranging from 10^{-7} to 10^{6} m and temporal scales of
925 minutes to hours or more. Sampling would have to encompass major cloud types, and several
926 coordinated aircraft would probably be required to provide an combination of remote-sensing
927 and *in situ* observations capable of resolving variations both vertically as well as horizontally
928 within and surrounding cloud systems. Variables identifying distinct cloud and meteorological
929 regimes, that could subsequently be mapped with space-based remote sensing, would be required
930 to allow the field results of be extrapolated to global scale and extended time periods. A future
931 study identifying the required variables, likely instruments to make the key measurements,
932 targeting requirements, and observation strategies aimed at reducing ACI modeling uncertainties
933 in general is indicated.

934

935 **6. Conclusions – A Three-Way Street**

936 The aerosol-related climate forcing uncertainties have not diminished appreciably in more than
937 20 years, despite substantial progress in other aerosol- and cloud-related measurement and
938 modeling areas. Forcing uncertainty translates directly into climate change attribution and
939 prediction uncertainty.

940 Unlike most previous reviews of aerosol climate forcing constraints and uncertainties, we take a
941 measurement-oriented perspective. As illustrated in Figure 1, the satellite and suborbital
942 measurement as well as the modeling research communities each have unique and essential
943 contributions to make to the other two to achieve substantial progress in reducing the uncertainty
944 in aerosol climate forcing overall. The application of loose satellite constraints on aerosol type
945 and precursor gas distributions to improve model simulations needs to be explored in broader
946 terms than previously, in part by taking the limited retrieved information content on particle size,
947 shape, and light-absorption where available and linking it to more specific aerosol species, based
948 on source properties projected to the observed locations by aerosol transport modeling. This is an
949 example of a two-way street – the models help refine the satellite-retrieved aerosol type results,
950 especially where the AOD is too low for reliable satellite aerosol-type retrieval or where cloud,
951 complex surface topography or snow cover entirely precludes remote-sensing aerosol
952 measurement; the aggregate of satellite instruments provides the 3-D spatial distribution of

aerosol amount and type to constrain and/or validate the models, improving aerosol source initialization, transport, transformation, and deposition, and reducing model bias. Aerosol data assimilation offers another example: for each analysis cycle, the model projects past observations into the future, which in turn provides additional constraints for the assimilation of new data.

As outlined in Section 4 above, for the suborbital component to adequately contribute to modeling and to the interpretation of satellite observations (the third way), a database of systematic, statistically representative *in situ* measurements needs to be developed, containing the key particle microphysical, optical, and chemical properties and associated uncertainty estimates that cannot be derived from remote-sensing measurements alone. Such *in situ* measurements are needed to improve assumptions and parameterizations in models as well as observation operators for data assimilation, putting the model-assumed aerosol particle properties on more solid and consistent footing. The detailed aerosol properties will also serve to improve the priors or constraints on satellite retrieval algorithms, adding value to more than two decades of retrospective as well as planned future satellite aerosol observations. Further, such *in situ* aerosol data, with attention to the co-variability among aerosol and meteorological variables, would make more precise and *quantitative* connections between the satellite optical constraints on aerosol amount and type and the modeled, species-specific, aerosol mass (e.g., the MEEs), a key requirement for data assimilation and model validation. A separate suborbital measurement program is needed to characterize the processes by which the aerosol particles and clouds interact, reporting detailed cloud properties in the presence of different aerosol amounts and types, under a range of meteorological conditions.

Completing the pattern of relationships, models, constrained by satellite measurements, can help in targeting the systematic *in situ* measurements to regions where they will matter most. Subsequently, models can help interpret the aerosol source and aging history, as well as cloud regime-type and evolution acquired through satellite and suborbital observations. In addition to its application to climate-related study, this approach would help improve model representation of surface-level particulate matter (PM) concentrations and composition, which is at the heart of air quality monitoring on regional and global scales (e.g., Appel et al., 2008; Hammer et al., 2019; van Donkelaar et al., 2021). Specifically, two leading sources of uncertainty for air quality applications relate to the aerosol vertical distribution and aerosol composition, which are also

among the leading uncertainties in aerosol contributions to climate forcing, though the observational requirements for air quality applications are somewhat different, e.g., requiring near-surface aerosol chemical toxicity and possibly tighter constraints on particle size. For air quality applications, recent advances in data analysis techniques are likely to make important contributions (e.g., Bellinger et al., 2017)

Clearly, programs supporting advanced, global-scale satellite and surface-based aerosol, precursor gas, and cloud observations, climate modeling, surface networks, and intensive field campaigns aimed at characterizing the underlying physical and chemical processes involved, as currently planned, are all essential. The main parts of the overall picture missing from current programs or those planned for the near future are: (1) a program of long-term, systematic aircraft measurements aimed at creating a climatology of the key aerosol microphysical properties driving aerosol-climate interactions for the major aerosol airmass types, along with their statistical distributions and uncertainties, (2) a suborbital program aimed at filling gaps in aerosol-cloud-interaction-related cloud-scale microphysics, cloud optical properties, and associated dynamics, and (3) the mandate, the support, and the computational resources for the respective communities to work together in detail on the *synthesis* effort – the three-way street (Figure 1). Such efforts would go a long way toward 'model-data fusion' (e.g., Gettelman et al., 2022); that is, developing consistent representations of aerosol properties as retrieved from remote sensing, measured *in situ*, and adopted by models (sometimes referred to in the AeroCom, AeroSat, and ICAP communities as "harmonizing" aerosol types among different platforms and communities). It would help members of the involved research communities agree upon those properties that most affect the aerosol analysis or application in a given place and time, and would greatly improve the feasibility of exchanging aerosol information among and between measurements and models. The cloud-related requirements for constraining aerosol-cloud interactions, such as better characterization of ice-cloud processes, documentation of aerosol effects on cloud condensate and cloud fraction, as well as vertical velocity constraints, especially in convective systems, are also needed. Yet, fully effecting the three-way street seems to be essential for substantially reducing the aerosol direct and indirect forcing uncertainty that persistently dominates climate and also affects air quality prediction uncertainty. The technical capabilities to achieve this are all currently available.

Acknowledgments

R. Kahn thanks the AeroCom and AeroSat communities for discussions over many years that helped refine many of the ideas presented in this paper, as well as the SAM-CAAM Science Definition Team for demonstrating that a notional payload of technologies available even in 2014 could meet the systematic aerosol *in situ* measurement requirements and fit within a relatively small aircraft. We also thank Yves Balkanski, Alan Brewer, Richard Ferrare, Bob Yokelson, and John Yorks for helpful notes related to their work, and three anonymous reviewers whose notes helped us improve the paper. AeroSat was initiated in the ESA Climate Change Initiative (CCI) project Aerosol_cci framework (ESA-ESRIN Contract no. 4000101545/10/I-AM), which also provides some AeroSat coordination support. R. Kahn is supported in part by NASA's Climate and Radiation Research and Analysis Program under Hal Maring, NASA's Atmospheric Composition Modeling and Analysis Program under Richard Eckman, and the NASA EOS MISR and Terra projects, E. Andrews is supported by NOAA cooperative agreement NA22OAR4320151. The National Center for Atmospheric Research is supported by the National Science Foundation. A. Nenes acknowledges support by the project PyroTRACH (ERC-2016-COG) funded from H2020-EU.1.1. - Excellent Science - European Research Council (ERC), project ID 726165 and from the European Union project FORCeS funded from Horizon H2020-EU.3.5.1 (project ID 821205). J.R. Pierce is supported by NASA grant 80NSSC21K0429. P. Stier acknowledges support from the European Research Council (ERC) project RECAP under the European Union's Horizon 2020 research and innovation programme (https://research-and-innovation.ec.europa.eu/funding/funding-opportunities/funding-programmes-and-open-calls/horizon-2020_en, last accessed April 2023) with grant agreement no. 724602, and the the FORCeS and NextGEMs project under the European Union's Horizon 2020 research programme with grant agreements 821205 and 101003470, respectively

We did not identify any conflicts-of-interest for any coauthor.

Open Research

1044 This paper represents a review and analysis of previously published work. As such, the
1045 underlying data are made available from the original sources through the cited literature.
1046
1047 **References**
1048
1049 Ackerman, A. S., Kirkpatrick, M. P., Stevens, D. E., & Toon, O. B. (2004). The impact of
1050 humidity above stratiform clouds on indirect aerosol climate forcing. *Nature 432*,
1051 doi:10.1038/nature03174.
1052
1053 Adebiyi, A.A., & Kok, J.F. (2020). Climate models miss most of the coarse dust in the
1054 atmosphere. Sci. Adv. 6, eaaz9507, doi:10.1126/sciadv.aaz9507.
1055
1056 Alvarado, M.J., Lonsdale, C.R., Macintyre, H.L., Bian, H., Chin, M., Ridley, D.A., et al. (2016).
1057 Evaluating model parameterizations of submicron aerosol scattering and absorption with *in situ*
1058 data from ARCTAS 2008. *Atmos. Chem. Phys., 16, 9435–9455*, doi:10.5194/acp-16-9435-2016.
1059
1060 Anderson, T.L., Charlson, R.J., Winker, D.M., Ogren, J.A., & Holmen, K. (2003). Mesoscale
1061 variations of tropospheric aerosols., J. Atmosph. Sci. 60, 119-135, doi:10.1175/1520-
1062 0469(2003)060.
1063
1064 Andreae, M.O. (2009). Correlation between cloud condensation nuclei concentration and
1065 aerosol optical thickness in remote and polluted regions. Atmos. Chem. Phys., 9, 543–556,
1066 doi:atmos-chem-phys.net/9/543/2009.
1067
1068 Andreae, M.O. (2019). Emission of trace gases and aerosols from biomass burning – an updated
1069 assessment. *Atmos. Chem. Phys., 19, 8523–8546*, doi:10.5194/acp-19-8523-2019.
1070
1071 Andrews, E., Sheridan, P.J., & Ogren, J.A. (2011). Seasonal differences in the vertical profiles of
1072 aerosol optical properties over rural Oklahoma. *Atmos. Chem. Phys. 11, 10661–10676*,
1073 doi:10.5194/acp-11-10661-2011.
1074

Andrews, E., Ogren, J.A., Kinne, S., & Samset, B. (2017). Comparison of AOD, AAOD and column single scattering albedo from AERONET retrievals and in situ profiling measurements. *Atmos. Chem. Phys., 17, 6041–6072*, doi:10.5194/acp-17-6041-2017.

Andrews, E., Sheridan, P.J., Ogren, J.A., Hageman, D., Jefferson, A., et al. (2019). Overview of the NOAA/ESRL Federated Aerosol Network. *Bull. Am. Meteorol. Soc. 123-135*, doi:10.1175/BAMS-D-17-0175.1.

Appel, K.W., Bhave, P.V., Gilliland, A.B., Sarwar, G., & Roselle, S.J. (2008). Evaluation of the community multiscale air quality (CMAQ) model version 4.5: Sensitivities impacting model performance; Part II—particulate matter. *Atmos. Env. 42, 6057-6066,* doi:10.1016/j.atmosenv.2008.03.036.

Balkanski, Y., Mona, L., Andrews, E., Bellouin, N., Carslaw, K., Chin, M., et al. (2021). AeroCom-AeroSat Commission on Constraining Aerosol Properties. AeroCom-AeroSat virtual meeting, 14 October 2021.

Bauer, S. E., Wright, D. L., Koch, D., Lewis, E. R., McGraw, R., Chang, L.-S., et al., (2008). MATRIX 534 (Multiconfiguration Aerosol TRacker of mIXing state): an aerosol microphysical module for 535 global atmospheric models. *Atmos. Chem. Phys. 8*(20*), 6003–6035*, doi:10.5194/acp-8-6003-2008.

Behrenfeld, M.J., Moore, R.H., Hostetler, C.A., Graff, J., Gaube, P, et al. (2019). The North Atlantic Aerosol and Marine Ecosystem Study (NAAMES): Science Motive and Mission Overview. *Front. Mar. Sci. 6, 122*, doi:10.3389/fmars.2019.00122.

Bellinger, C., Jabbar, M.S.M, Zaiane, O., & Osornio-Vargas, A. (2017). A systematic review of data mining and machine learning for air pollution epidemiology. *BMC Public Health 17 (907)*, doi:10.1186/s12889-017-4914-3.

Bellouin, N., Quaas, J., Gryspeerdt, E., Kinne, S., Stier, P., Watson-Parris, D., Boucher, O., et al. (2020). Bounding global aerosol radiative forcing of climate change. *Rev. Geophys. 58(1), e2019RG000660*, doi:10.1029/2019RG000660.

Benedetti, A., Morcrette, J.-J., Boucher, O., Dethof, A., Engelen, R. J., Fisher, M., et al. (2009). Aerosol analysis and forecast in the European Centre for Medium-Range Weather Forecasts Integrated Forecast System: 2. Data assimilation. *J. Geophys. Res., 114, D13205*, doi:10.1029/2008JD011115.

Bian, H., Chin, M., Hauglustaine, D. A., Schulz, M., Myhre, G., Bauer, S. E., et al. (2017). Investigation of global particulate nitrate from the AeroCom phase III experiment. *Atmos. Chem. Phys. 17, 12911–12940*. doi:10.5194/acp-17-12911-2017.

Boucher, O., Randall, D., Artaxo, P., Bretherton, C., Feingold, G., Forster, P., et al. (2013). Clouds and Aerosols. Climate Change 2013: The Physical Science Basis. Contribution of Working Group I to the Fifth Assessment Report of the Intergovernmental Panel on Climate Change [Stocker, T.F., Qin, D., Plattner, G.-K., Tignor, M., Allen, S.K., Boschung, J., et al. (eds.)]. Cambridge University Press, Cambridge, United Kingdom and New York, NY, USA.

Bougiatioti, A., Nenes, A., Lin, J.J., Brock, C.A., de Gouw, J., Liao, J., et al. (2020). Drivers of cloud droplet number variability in the summertime with focus on the Southeast United States. *Atmos.Chem.Phys 20, 12163–12176*, doi:10.5194/acp-20-12163-2020.

Bretherton, C.S., Wood, R., George, R.C., Leon, D., Allen, G., & Zhent, X. (2010). Southeast Pacific stratocumulus clouds, precipitation and boundary layer structure sampled along 20 S during VOCALS-Rex. *Atmos. Chem. Phys., 10, 10639–10654*, doi: 10.5194/acp-10-10639-2010.

Bretherton, C. S., Blossey, P. N., and Uchida, J.: Cloud droplet sedimentation, entrainment efficiency, and subtropical stratocumulus albedo, *Geophys. Res. Lett., 34, L03813*, doi:10.1029/2006GL027648.

Brock, C.A., Froyd, K.S., Dollner, M., Williamson, C.J., Schill, G., Murphy, D.M., et al. (2021). Ambient aerosol properties in the remote atmosphere from global-scale in situ measurements, *Atmos. Chem. Phys., 21, 15023–15063,* doi:10.5194/acp-21-15023-2021.

Buchard, V., Randles, C.A., Silva, A.M. da, Darmenov, A., Colarco, P.R., Govindaraju, et al. (2017). The MERRA-2 aerosol aeanalysis, 1980 onward. Part II: Evaluation and case studies. *J. Clim. 30, 6851–6872*, doi:10.1175/JCLI-D-16-0613.1.

Burgos, M.A., Andrews, E., Titos, G., Benedetti, A., Bian, H., Buchard, V., et al. (2020). A global model–measurement evaluation of particle light scattering coefficients at elevated relative humidity. *Atmos. Chem. Phys., 20, 10231–10258*, doi:10.5194/acp-20-10231-2020.

Burton, S.P., Ferrare, R.A., Hostetler, C.A., Hair, J.W., Rogers, R.R., Obland, M.D., et al. (2012). Aerosol classification using airborne High Spectral Resolution Lidar measurements – methodology and examples. *Atmos. Meas. Tech. 73–98*, doi:10.5194/amt-5-73-2012.

Burton, S.P., Hair, J.W., Kahnert, M., Ferrare, R.A., Hostetler, C.A., Cook, A.L., et al. (2015). Observations of the spectral dependence of linear particle depolarization ratio of aerosols using NASA Langley airborne High Spectral Resolution Lidar. Atmos. Chem. Phys., 15, 13453–13473, doi:10.5194/acp-15-13453-2015.

Cao, Y., Zhu, Y., Wang, M., Rosenfeld, D., Liang, Y., Liu, J., et al. (2023). Emission reductions significantly reduce the hemispheric contrast in cloud droplet number concentration in recent two decades. *J. Geophys. Res. Atmosph. 128, e2022JD037417*, doi:10.1029/2022JD037417.

Capelle, V., Chedin, A., Pondrom, M., Crevoisier, C., Armante, R., et al. (2018). Infrared dust aerosol optical depth retrieved daily from IASI and comparison with AERONET over the period 2007–2016. Remt. Sens. Env. 206, 15-32, doi:10.1016/j.rse.2017.12.008.

1165 Carr, J.L., Á. Horváth, D.L. Wu, & M.D. Friberg (2022). Stereo plume height and motion
1166 retrievals for the record-setting Hunga Tonga-Hunga Ha'apai eruption of 15 January 2022.
1167 *Geophys. Res. Lett. 49, e2022GL098131*, doi:10.1029/2022GL098131
1168
1169 Carslaw, K.S., Lee, L.A., Reddington, C.L., Pringle, K.J., Rap, A., Forster, P.M., et al. (2013).
1170 Large contribution of natural aerosols to uncertainty in indirect forcing. *Nature 503, 67-74*,
1171 doi:10.1038/nature12674.
1172
1173 Carslaw, K.S., Gordon, H., Hamilton, D.S., Johnson, J.S., Regayre, L.A., et al. (2017). Aerosols
1174 in the pre-industrial atmosphere. *Curr. Clim Change Rep. 3, 1-15*, doi:10.1007/s40641-017-
1175 0061-2.
1176
1177 CCSP (U.S. Climate Change Science Program) Synthesis and Assessment Product 2.3 (2009).
1178 Atmospheric aerosol properties and climate impacts. Chin, M., R.A. Kahn, & S. Schwartz, Eds.
1179 Pp. 116.
1180
1181 Chin, M., Ginoux, P., Kinne, S.,Torres, O., Holben, Duncan, B.N., et al. (2002). Tropospheric
1182 aerosol optical thickness from the GOCART model and comparisons with satellite and sun
1183 photometer measurements. *J. Atmos. Sci. 59 (3)*, doi:10.1175/1520-0469(2002).
1184
1185 Christensen, M., Gettelman, A., Cermak, J., Dagan, G., Diamond, M., Douglas, A., et al. (2022).
1186 Opportunistic experiments to constrain aerosol radiative forcing. *Atmos. Chem. Phys. 22, 641–*
1187 *674*, doi: 10.5194/acp-22-641-2022.
1188
1189 Colarco, P.R., Nowottnick, E.P., Randles, C.A., Yi, B., Yang, P., Kim, K-M., et al. (2013).
1190 Impact of radiatively interactive dust aerosols in the NASA GEOS-5 climate model: Sensitivity
1191 to dust particle shape and refractive index. *J. Geophys. Res. Atmos.,119, 753–786*,
1192 doi:10.1002/2013JD020046.
1193

1194 Crosbie, E., Ziemba, L.D., Shook, M.A., Robinson, C.E., Winstead, E.L., et al. (2022).
1195 Measurement report: Closure analysis of aerosol–cloud composition in tropical maritime warm
1196 convection. *Atmos. Chem. Phys., 22, 13269–13302*, doi:10.5194/acp-22-13269-2022.
1197
1198 Das, S., Harshvardhan, H., Bian, H., Chin, M., Curci, G., et al. (2017), Biomass burning aerosol
1199 transport and vertical distribution over the South African-Atlantic region. *J. Geophys. Res.*
1200 *Atmos., 122, 6391–6415*, doi:10.1002/2016JD026421.
1201
1202 Dawson, K.W., Meskhidze, N., Burton, S.P., Johnson, M.S., Kacenelenbogen, M.S., Hostetler,
1203 C.A., & Hu, Y. (2017). Creating Aerosol Types from Chemistry (CATCH): A new algorithm to
1204 extend the link between remote sensing and models. *J. Geophys. Res., Atmos. 122, 12,366–*
1205 *12,392*, doi:10.1002/2017JD026913.
1206
1207 Dagan, G. & P. Stier (2020). Constraint on precipitation response to climate change by
1208 combination of atmospheric energy and water budgets. *npj Clim. Atmos. Sci. 3 (34)*.
1209 doi:10.1038/s41612-020-00137-8.
1210
1211 Dadashazar, H., Wnag, Z., Crosbie, E., Brunke, M., Zeng, X., et al. (2017). Relationships
1212 between giant sea salt particles and clouds inferred from aircraft physicochemical data. *J.*
1213 *Geophys. Res. Atmos., 122, 3421–3434*, doi:10.1002/2016JD026019.
1214
1215 Dawson, K.W., Ferrare, R.A., Moore, R.H., Clayton, M.D., Thorsen, T.J., & Eloranta, E.W.
1216 (2020). Ambient aerosol hygroscopic growth from combined Raman lidar and HSRL. *J.*
1217 *Geophys. Res. Atmos. 125, e2019JD031708*, doi:10.1029/2019JD031708.
1218
1219 Dee, D.P., S.M. Uppala, A.J. Simmons, P. Berrisford, P. Poli, S. Kobayashi, U., et al. (2011).
1220 The ERA-Interim reanalysis: configuration and performance of the data assimilation system. *Q.*
1221 *J. Royal Met. Soc. 137 (656), 553-597*, doi:10.1002/qj.828.
1222

de Leeuw, G., Andreas, E.L., Anguelova, M.D., Fairall, C.W., Lewis, E.R., O'Dowd, C., Schulz, M., &. Schwartz S.E. (2011). Production flux of sea spray aerosol. *Rev. Geophys. 49, RG2001*, doi:10.1029/2010RG000349.

Denjean, C., Formenti, P., Desboeufs, K., Desboeufs, K., Chevaillier, S., Triquet, S., et al. (2016). Size distribution and optical properties of African mineral dust after intercontinental transport. *J. Geophys. Res. Atmos., 121, 7117–7138*, doi:10.1002/2016JD024783.

Di Biagio, C., Formenti, P., Balkanski, Y., Caponi, L., Cazaunau, M., Pangui, E., et al. (2017). Global scale variability of the mineral dust long-wave refractive index: a new dataset of in situ measurements for climate modeling and remote sensing. *Atmos. Chem. Phys., 17, 1901–1929*, doi:10.5194/acp-17-1901-2017.

Dubovik, O., Lapyonok, T., Kaufman, Y.J., Chin, M., Ginoux, P., Kahn, R.A., & Sinyuk, A., (2008). Retrieving global sources of aerosols from satellites using inverse modeling. *Atmos. Chem. Phys. 8*, 209-250, doi:10.5194/ACP-8-209-2008.

Dubovik, O., Herman, M., Holdak, A., Lapyonok, T., Tanre, D., Deuze, J.L., et al. (2011). Statistically optimized inversion algorithm for enhanced retrieval of aerosol properties from spectral multi-angle polarimetric satellite observations. *Atmos. Meas. Tech. 4, 975–1018,* doi: 10.5194/amt-4-975-2011.

Ervens, B., Feingold, G., & Kreidenweis, S. M. (2005). The influence of water-soluble organic carbon on cloud drop number concentration. *J. Geophys. Res., 110, D18211*, doi:10.1029/2004JD005634.

Fanourgakis, G. S., Kanakidou, M., Nenes, A., Bauer, S.E., Bergman, T., Carslaw, K.S., et al. (2019). Evaluation of global simulations of aerosol particle and cloud condensation nuclei number, with implications for cloud droplet formation *Atmos. Chem. Phys., 19, 8591–8617*, doi: 10.5194/acp-19-8591-2019.

1254 Fast, J.D., Bell, D.M., Liu, J., Mei, F., Saliba, G., Shilling, J.E., et al. (2022). Using aircraft
1255 measurements to characterize subgrid-scale variability of aerosol properties near the ARM
1256 Southern Great Plains site. *Atmos. Chem. Phys., 22, 11217–11238,* doi:10.5194/acp-22-11217-
1257 2022.
1258
1259 Feingold, G., Yang, S., Hardesty, R.M., & Cotton, W.R. (1998). Feasibility of retrieving cloud
1260 condensation nucleus properties from doppler cloud radar, microwave radiometer, and lidar. *J.*
1261 *Atmos. Ocean Tech. 15, 1188-1195*. doi:10.1175/1520-0426.
1262
1263 Feingold, G., Cotton, W.R., Kreidenweis, S.M., & Davis, J.T. (1999). Impact of giant cloud
1264 condensation nuclei on drizzle formation in marine stratocumulus: Implications for cloud
1265 radiative properties. *J. Atmos. Sci., 56, 4100-4117*, doi:10.1175/1520-0469.
1266
1267 Feingold, G., Eberhard, W.L., Veron, D.E. & Previdi, M. (2003). First measurements of the
1268 Twomey aerosol indirect effect using ground-based remote sensors. *Geophys. Res. Lett., 30 (6),*
1269 *1287*, doi:10.1029/2002GL016633.
1270
1271 Feingold, G. (2003). Modeling of the first indirect effect: Analysis of measurement requirements.
1272 *Geophys. Res. Lett., 30 (19) 1997*, doi:10.1029/2003GL017967.
1273
1274 Fiedler, S., Kinne, S., Huang, W.T.K., Räisänen, P., O'Donnell, D., Bellouin, N., et al. (2019).
1275 Anthropogenic aerosol forcing – insights from multiple estimates from aerosol-climate models
1276 with reduced complexity. *Atmos. Chem. Phys., 19, 6821–6841*, doi: 10.5194/acp-19-6821-2019.
1277
1278 Flower, V.J.B., & Kahn, R.A. (2020a). Interpreting the volcanological processes of Kamchatka,
1279 based on multi-sensor satellite observations. *Remote Sens. Environ. 237, 111585*,
1280 doi:10.1016/j.rse.2019.111585.
1281
1282 Flower, V.J.B., & Kahn, R.A. (2020b). The evolution of Iceland volcano emissions, as observed
1283 from space. *J. Geophys. Res., 125, e2019JD031625*, doi:10.1029/2019JD031625.
1284

1285 Forster, P., Storelvmo, T., Armour, K., Collins, W., Dufresne, J.-L., Frame, D., et al. (2021). The
1286 Earth's Energy Budget, Climate Feedbacks, and Climate Sensitivity. In Climate Change 2021:
1287 The Physical Science Basis. Contribution of Working Group I to the Sixth Assessment Report of
1288 the Intergovernmental Panel on Climate Change [Masson-Delmotte, V., Zhai, P., Pirani, A.,
1289 Connors, S.L., Péan, C., Berger, S., et al. (eds.)]. *Cambridge University Press, Cambridge,*
1290 *United Kingdom and New York, NY, USA, pp. 923–1054*, doi:10.1017/9781009157896.009.
1291
1292 Foskinis, R., Nenes, A., Papayannis, A., Georgakaki, P., Kokkalis, P., Eleftheriadis, E.,
1293 Komppula, M., Vratolis, S., Soupiona, O., Gini, M., Vakkari, V., Tombrou, M., & Bossioli, E.
1294 (2022). Towards reliable retrievals of cloud droplet number for non-precipitating planetary
1295 boundary layer clouds and their susceptibility to aerosol. *Front. Remote Sens., 3:958207*.
1296 doi:10.3389/frsen.2022.958207.
1297
1298 Fougnie, B., Chimot, J., Vazques-Navarro, M., Marbach, T., & Bojkov, B. (2020). Aerosol
1299 retrieval from space –how does geometry of acquisition impact our ability to characterize aerosol
1300 properties. *J. Quant. Spect. & Radiative Transf. 256, 107304*, doi: 10.1016/j.jqsrt.2020.107304.
1301
1302 Gasteiger, J. & Wiegner, M. (2018). MOPSMAP v1.0: a versatile tool for the modeling of
1303 aerosol optical properties. *Geosci. Model Dev., 11, 2739–2762*, doi:10.5194/gmd-11-2739-2018.
1304
1305 Gelaro, R., McCarty, W., Suárez, M.J., Todling, R., Molod, A., Takacs, L., et al. (2017). The
1306 Modern-Era Retrospective Analysis for Research and Applications, Version 2 (MERRA-2). *J.*
1307 *Clim. 30, 5419–5454*. doi:10.1175/JCLI-D-16-0758.1.
1308
1309 Georgakaki, P., Bougiatioti, A., Wieder, J., Mignani, C., Ramelli, F., Kanji, Z.A., et al. (2021).
1310 On the drivers of droplet variability in Alpine mixed-phase clouds. *Atmos. Chem. Phys., 21,*
1311 *10993–11012*, doi:10.5194/acp-21-10993-2021.
1312
1313 Gettelman, A., Liu, X., Barahona, D., Lohmann, U., & Chen, C.C. (2012). Climate Impacts of
1314 Ice Nucleation. *J. Geophys. Ress 117, D20201*, doi:10.1029/2012JD017950.
1315

Gettelman, A., & Sherwood, S.C. (2016). Processes Responsible for Cloud Feedback. *Curr. Clim. Change Rep. 2, 179–189*, doi:10.1007/s40641-016-0052-8.

Gettelman, A., Geer, A.J., Forbes, R.M., Carmichael, G.R., Feingold, G., Posselt, D.J., et al. (2022). The Future of Earth System Prediction: Advances in Model-Data Fusion. *Science Advances 8 (14): eabn3488*, doi:10.1126/sciadv.abn3488.

Ghan, S., Guzman, G., and Abdul-Razzak, H. (1998). Competition between sea salt and sulfate particles as cloud condensation nuclei. *J. Atmos. Sci., 55, 3340–3347*, doi:10.1175/1520-0469.

Glassmeier, F., Hoffmann, F., Johnson, J.S., Yamaguchi, T., Carslaw, K.S., & Feingold, G. (2021). Ship-track-based assessments overestimate the cloud-mediated cooling effect of anthropogenic aerosol. *Science, 371, 485 – 489*, doi:10.1126/science.abd3980.

Gliß, J., Mortier, A., Schulz, M., Andrews, E., Balkanski, Y., Bauer, S.E., et al. (2021). AeroCom phase III multi-model evaluation of the aerosol life cycle and optical properties using ground- and space-based remote sensing as well as surface in situ observations. *Atmos. Chem. Phys. 21, 87–128*. doi:10.5194/acp-21-87-2021.

Go, S., Kima, J., Mok, J., Irie, H., Yoon,J., Torres, O., et al. (2020). Ground-based retrievals of aerosol column absorption in the UV spectral region and their implications for GEMS measurements. *Remt. Sens. Env. 245, 111759*, doi: 10.1016/j.rse.2020.111759.

Gonzalez, M.E., Corral, A.F., Crosbie, E., Dadazhazar, H., Diskin, G.S., et al. (2022). Relationships between supermicrometer particle concentrations and cloud water sea salt and dust concentrations: analysis of MONARC and ACTIVATE data. *Environ. Sci. Atmosph. 2, 738*, doi: 10.1039/d2ea00049k.

Gordon, T.D., Wagner, N.L., Richardson, M.S., Law, D.C., Wolfe, D., Eloranta, E.W., et al. (2015). Design of a novel open-path aerosol extinction cavity ringdown spectrometer. *Aerosol Sci. Tech., 49:9, 717-726*, doi:10.1080/02786826.2015.1066753.

Griffin, D., Sioris, C., Chen, J., Dickson, N., Kovachik, A., deGraaf, M., et al. (2020). The 2018 fire season in North America as seen by TROPOMI: aerosol layer height validation and evaluation of model-derived plume heights. *Atmos. Meas. Tech. 13, 1427–1445*, doi:10.5194/amt-13-1427-2020.

Grosvenor, D. P., Sourdeval, O., Zuidema, P., Ackerman, A., Alexandrov, M. D., Bennartz, R., et al. (2018). Remote sensing of droplet number concentration in warm clouds: A review of the current state of knowledge and perspectives. *Rev. Geophys. 56*, doi:10.1029/2017RG000593.

Gryspeerdt, E., Goren, T., Sourdeval, O., Quaas, J., Mülmenstädt, J., Dipu, S., Unglaub, C., Gettelman, A., and Christensen, M. (2019). Constraining the aerosol influence on cloud liquid water path. *Atmos*. *Chem. Phys., 19, 5331–5347*, doi:10.5194/acp-19-5331-2019.

Gryspeerdt, E., Goren, T., & Smith, T.W.P. (2021). Observing the timescales of aerosol–cloud interactions in snapshot satellite images. *Atmos. Chem. Phys., 21, 6093–6109*, doi:10.5194/acp-21-6093-202.1.

Guimond, S.R., Tian, L., Heymsfield, G.M., & Fraiser, S.J. 2014. Wind retrieval algorithms for the IWRAP and HIWRAP airborne doppler radars with applications to hurricanes. *J. Atmos. Ocean Tech. 31, 1189-1214*, doi:10.1175/JTECH-D-13-00140.1.

Gupta, P., Levy, R.C., Mattoo, S., Remer, L.A., Holz, R.E., & Heidinger, A.K. (2019). Applying the Dark Target aerosol algorithm with Advanced Himawari Imager observations during the KORUS-AQ field campaign. *Atmos. Meas. Tech., 12, 6557–6577*, doi:10.5194/amt-12-6557-2019.

Hamilton, D.S., Hantson, S., Scott, C.E., Kaplan, J.O., Pringle, K.J., et al. (2018). Reassessment of pre-industrial fire emissions strongly affects anthropogenic aerosol forcing. *Nat. Comm. 9, 3182*, doi:10.1038/s41467-018-05592-9.

Hammer, M.S., van Donkelaar, A., Martin, R.V., Li, C., Lyapustin, A., Sayer, A.M., Hsu, C.N., et al. (2019). Improved global estimates of fine particulate matter concentrations and trends derived from updated satellite retrievals, modeling advances, and additional ground-based monitors. *Environ. Sci. Tech. 54, 7879−7890*, doi:10.1021/acs.est.0c01764.

Hasekamp, O.P., Litvinov, P., & A. Butz, A. (2011). Aerosol properties over the ocean from PARASOL multiangle photopolarimetric measurements. *J. Geophys. Res. 116, D14204*, doi:10.1029/2010JD015469.

Haywood, J.M., Ramaswamy, V., & Donner, L.J. (1997). A limited-area-model case study of the effects of sub-grid scale Variations in relative humidity and cloud upon the direct radiative forcing of sulfate aerosol. *Geophys. Res. Lett. 24, 143-146*, doi: 10.1029/96GL03812.

Held, I.M., and Soden, B.J. (2006). Robust responses of the hydrological cycle to global warming. *J. Clim. 19, 5686-5698*, doi: 10.1175/JCLI3990.1.

Hélière, A., Gelsthorpe, R., Le Hors, L., & Toulemont, Y. (2012). ATLID, the atmospheric lidar on board the Earthcare Satellite. *Proc. SPIE 10584, 105842D*. doi:10.1117/12.2309095.

Hess, M., Koepke, P., & Schult, I. (1998). Optical Properties of Aerosols and Clouds: The software package OPAC. *Bull. Am. Met. Soc. 79, 831-844*, doi: 10.1175/1520-0477(1998)079.

Hoesly, R.M., Smith, S.J., Feng, L., Klimont, Z., Janssens-Maenhout, G., Bolt, R.M., et al. (2018). Historical (1750–2014) anthropogenic emissions of reactive gases and aerosols from the Community Emissions Data System (CEDS). *Geosci. Model Dev., 11, 369–408*, doi:10.5194/gmd-11-369-2018.

Holben, B. N., Eck, T. F., Slutsker, I., Tanré, D., Buis, J. P., Setzer, A., et al. (1998). AERONET — A federated instrument network and data archive for aerosol characterization *Remt. Sens. Environ., 66, 1–16*, doi:10.1016/S0034-4257(98)00031-5.

Holzer-Popp, T., de Leeuw, G., Griesfeller, J., Martynenko, D., Kluser, L., Bevan, S., et al. (2013). Aerosol retrieval experiments in the ESA Aerosol cci project. *Atmos. Meas. Tech., 6, 1919–1957*, doi: 10.5194/amt-6-1919-2013.

Huneeus, N., Schulz, M.,. Balkanski, Y., Griesfeller, J., Prospero, J.A., Kinne, S., et al. (2011). Global dust model intercomparison in AeroCom Phase I. *Atmos. Chem. Phys., 11, 7781– 7816*, doi:10.5194/acp-11-7781-2011.

Iacono, M.J., Delamere, J.S., Mlawer, E.J., Shephard, M.W., Clough, S.A., & Collins, W.D. (2008). Radiative forcing by long-lived greenhouse gases: Calculations with the AER radiative transfer models. *J. Geophys. Res. 113, no. D13103*, doi:10.1029/2008JD009944.

Ichoku, C., & Ellison, L. (2014), Global top- down smoke- aerosol emissions estimation using satellite fire radiative power measurements. *Atmos. Chem. Phys., 14, 6, 643– 6,667*, doi: 10.5194/acp-14-6643-2014.

IPCC (2013). Summary for Policymakers. In: Climate Change 2013: The Physical Science Basis. Contribution of Working Group I to the Fifth Assessment Report of the Intergovernmental Panel on Climate Change [Stocker, T.F., Qin, D., Plattner, G.-K., Tignor, M., Allen, S.K., Boschung, J., et al. (eds.)]. Cambridge University Press, Cambridge, United Kingdom and New York, NY, USA.

Jenkins, S., Povey, A., Gettelman, A., Grainger, R., Stier, P., & Allen, M. (2022). Is anthropogenic global warming accelerating?. *J. Clim. 35, 4273-4290*, doi:10.1175/JCLI-D-22-0081.1.

Jeong, M-J., & Hsu, N.C. (2008). Retrievals of aerosol single-scattering albedo and effective aerosol layer height for biomass-burning smoke: Synergy derived from “A-Train” sensors. *Geophys. Res. Lett. 35, L24801*, doi:10.1029/2008GL036279.

Jiang, H., & Feingold, G. (2006). Effect of aerosol on warm convective clouds: Aerosol-cloudsurface flux feedbacks in a new coupled large eddy model. *J. Geophys. Res., 111, D01202*, doi:10.1029/2005JD006138.

Jung, E., Albrecht, B.A., Jonsson, H.H., Chen, Y.-C., Seinfeld, J.H., et al. (2015). Precipitation effects of giant cloud condensation nuclei artificially introduced into stratocumulus clouds. *Atmos. Chem. Phys., 15, 5645–5658*, doi:10.5194/acp-15-5645-2015.

Junghenn Noyes, K.T., Kahn, R.A., Sedlacek, A., Kleinman, L., Limbacher, J., Li, Z. (2020). Wildfire smoke particle properties and evolution, from space-based multi-angle imaging. *Remote Sens. 12, 769*, doi:10.3390/rs12050769.

Junghenn Noyes, K.T., Kahn, R.A., Limbacher, J.A., & Li, Z. (2022). Canadian and Alaskan wildfire smoke particle properties, their evolution, and controlling factors, using satellite observations. *Atmos. Chem. Phys. 22, 10267–10290,* doi:10.5194/acp-22-10267-2022.

Kacarab, M., Thornhill, K.L., Dobracki, A., Howell, S.G., O'Brien, J.R., Freitag, S., et al. (2020). Biomass burning aerosol as a modulator of droplet number in the southeast Atlantic region. *Atmos. Chem. Phys., 20, 3029–3040*, doi:10.5194/acp-20-3029-2020.

Kahn, R.A., Ogren, J.A., Ackerman, T.P., Bosenberg, J., Charlson, R.J., Diner, D.J., et al. (2004). Aerosol data sources and their roles within PARAGON, *Bull. Am. Met. Soc. 85, 1511-1522*, doi:10.1175/BAMS-85-10-1511.

Kahn, R.A., Chen, Y., Nelson, D.L., Leung, F-Y., Li, Q., Diner, D.J., & Logan, J.A. (2008). Wildfire smoke injection heights – Two perspectives from space. *Geophys. Res. Lett. 35,* doi:10.1029/2007GL032165.

Kahn, R.A. (2012). Reducing the uncertainties in direct aerosol radiative forcing. *Surv. Geophys. 33, 701–721*, doi:10.1007/s10712-011-9153-z.

Kahn, R.A., & Gaitley, B.J. (2015). An analysis of global aerosol type as retrieved by MISR. *J. Geophys. Res. Atmos. 120*, *4248-4281*, doi:10.1002/2015JD023322.

Kahn, R.A., Berkoff, T., Brock, C., Chen, G., Ferrare, R., Ghan, S., et al. (2017). *SAM-CAAM*: A concept for acquiring systematic aircraft measurements to characterize aerosol air masses. *Bull. Am. Meteoro. Soc. 2215-2228*, doi:10.1175/BAMS-D-16-0003.1.

Kahn, R.A., & Samset, B.H. (2022). Ch. 10, Remote sensing measurements of aerosol properties. In: Aerosols and Climate, K.S. Carslaw, Ed., Elsevier Publications, ISBN: 978-0-12-819766-0, pp. 823.

Kalashnikova, O.V., Garay, M.J., Martonchik, J.V., & Diner, D.J. (2013). MISR Dark Water aerosol retrievals: operational algorithm sensitivity to particle non-sphericity. *Atmos. Meas. Tech., 6, 2131–2154*, doi:10.5194/amt-6-2131-2013.

Kapustin, V.N., Clarke, A.D., Shinozuka, Y., Howell, S., Brekhovskikh, V., Nakajima, T., & Higurashi, A. (2006). On the determination of a cloud condensation nuclei from satellite: Challenges and possibilities*, J. Geophys. Res., 111, D04202*, doi:10.1029/2004JD005527.

Kim, D., M. Chin, M., Yu, H., Diehl, T., Tan, Q., Kahn, R.A., et al. (2014). Sources, sinks, and transatlantic transport of North African dust aerosol: A multi-model analysis and comparison with remote sensing data*. J. Geophys. Res. 119*, *6259-6277*, doi:10.1002/2013JD021099.

Kim, D., Chin, M., Yu, H., Pan, X., Bian, H., Tan, Q.,et al. (2019). Asia and trans-Pacific Dust: A multi-model and multi-remote sensing observation analysis. *J. Geophys. Res. 124*, doi:10.1029/2019JD030822.

Kim, M-H., Omar, A.H., Tackett, J.L., Vaughan, M.A., Winker, D.M., Trepte, C.R., et al. (2018). The CALIPSO version 4 automated aerosol classification and lidar ratio selection algorithm. *Atmos. Meas. Tech. 11, 6107–6135*, doi: 10.5194/amt-11-6107-2018.

1501 Kinne, S., Lohmann, U., Feichter, J., Timmreck, C., Schulz, M., Ghan, S., et al. (2003). Monthly
1502 Averages of Aerosol Properties: A Global comparison among models, satellite data and
1503 AERONET ground data. *J. Geophys. Res, 108, 4634*. doi: 10.1029/2001JD001253.
1504
1505 Kinne, S., Schulz, M., Textor, C., Guibert, S., Balkanski, Y., Bauer, S. E., et al. (2006). An
1506 AeroCom initial assessment – optical properties in aerosol component modules of global models.
1507 *Atmos. Chem. Phys., 6, 1815–1834*. doi:10.5194/acp-6-1815-2006.
1508
1509 Kleinman, L. I., Sedlacek III, A. J., Adachi, K., Buseck, P. R., Collier, S., Dubey, M. K., et al.
1510 (2020). Rapid evolution of aerosol particles and their optical properties downwind of wildfires in
1511 the western US. *Atmos. Chem. Phys., 20, 13319–13341*, doi:10.5194/acp-20-13319-2020.
1512
1513 Koch, D, Schulz, M., Kinne, S., McNaughton, C., Spackman, J.R., Balkanski, Y., et al. (2009).
1514 Evaluation of black carbon estimations in global aerosol models. *Atmos. Chem. Phys., 9, 9001–*
1515 *9026*, doi:10.5194/acp-9-9001-2009.
1516
1517 Kokkola, H, T. Kühn, A. Laakso, T. Bergman, K.E.J. Lehtinen, T. Mielonen, A. (2018).
1518 SALSA2.0: The sectional aerosol module of the aerosol–chemistry–climate model
1519 ECHAM6.3.0-HAM2.3-MOZ1.0. *Geosci. Model Dev., 11, 3833–3863*, doi: 10.5194/gmd-11-
1520 3833-2018.
1521
1522 Koren, I., Kaufman, Y.J., Remer, L.A., Martins, J.V. (2004). Measurement of the effect of
1523 Amazon smoke on inhibition of cloud formation. *Science, 303, 1342–1345*, doi:
1524 10.1126/science.1089424.
1525
1526 Koren, I., Kaufman, Y.J., Rosenfeld, D., Remer, L.A., & Rudich, Y. (2005). Aerosol
1527 invigoration and restructuring of Atlantic convective clouds. *Geophys. Res. Lett.,32, L14828*,
1528 doi:10.1029/2005GL023187.
1529
1530 Koren, I., Remer, L.A., Kaufman, Y.J., Rudich, Y., and Martins, J.V. (2007). On the twilight
1531 zone between clouds and aerosols. *Geophys. Res. Lett 34, L08805*, doi: 10.1029/2007GL029253.

Kylling, A., Vandenbussche, S., Capelle, V., Cuesta, J., Klüser, L., Lelli, L., et al. (2018). Comparison of dust layer heights from active and passive satellite sensors, *Atmos. Meas. Tech. 11, 2911-2936*, doi:10.5194/amt-11-2911-2018.

Laj, P., Bigi, A., Rose, C., Andrews, E., Myhre, C.L., Coen, M.C., et al. (2020). A global analysis of climate-relevant aerosol properties retrieved from the network of Global Atmosphere Watch (GAW) near-surface observatories. *Atmos. Meas. Tech., 13, 4353–4392*, doi:10.5194/amt-13-4353-2020.

Lau, K. M., Ramanathan, V., Wu, G.-X., Li, Z., Tsay, S. C., and Hsu, C.N. (2008). The joint aerosol-monsoon experiment: a new challenge for monsoon climate research. *Bull. Am. Meteorol. Soc. 89, 369–383*. doi:10.1175/BAMS-89-3-369

Lee, C.M., Cable, M.L., Hook, S.J., Green, R.O., Ustin, S.L., Mandl, D.J., & Middleton, E.M. (2015). An introduction to the NASA Hyperspectral InfraRed Imager (HyspIRI) mission and preparatory activities. *Remt. Sens. Environ. 167, 6-19*, doi:10.1016/j.rse.2015.06.012.

Lee, J.-Y., Marotzke, J., Bala, G., Cao, L., Corti, S., Dunne, J.P., et al. (2021). Future Global Climate: Scenario-Based Projections and Near- Term Information. In Climate Change 2021: The Physical Science Basis. Contribution of Working Group I to the Sixth Assessment Report of the Intergovernmental Panel on Climate Change [Masson-Delmotte, V., Zhai, P., Pirani, A., Connors, S.L., Péan, C., Berger, S., et al. (eds.)]. *Cambridge University Press, Cambridge, United Kingdom and New York, NY, USA, pp. 553–672*, doi:10.1017/9781009157896.006.

Lee, S.S., Feingold, G., McComiskey, A., Yamaguchi, T., Koren, I., Martins, J.V., & H. Yu, H. (2014), Effect of gradients in biomass burning aerosol on shallow cumulus convective circulations. *J. Geophys. Res. Atmos., 119, 9948–9964*, doi:10.1002/2014JD021819.

1561 Levy, R. C., Remer, L. A., & Dubovik, O. (2007). Global aerosol optical properties and
1562 application to Moderate Resolution Imaging Spectroradiometer aerosol retrieval over land*, J.*
1563 *Geophys. Res. Atmos., 112, D13210*, doi:10.1029/2006JD007815.
1564
1565 Li, S., Kahn, R.A., Chin, M., Garay, M.J., & Liu, Y. (2015). Improving satellite-retrieved aerosol
1566 microphysical properties using GOCART data. *Atmos. Meas. Tech. 8, 1157–1171*.
1567 doi:10.5194/amt-8-1157-2015.
1568
1569 Li, J., Kahn, R. A., Wei, J., Carlson, B.E., Lacis, A. A., Li, Z., et al. (2020). Synergy of satellite-
1570 and ground-based aerosol optical depth measurements using an ensemble Kalman filter
1571 approach. *J. Geophys. Res. Atmos. 125, e2019JD031884*, doi:10.1029/2019JD031884.
1572
1573 Li, J., Carlson, B.E., Yung, Y.L., Lv, D., Hansen, J.E., Penner, J.E., et al. (2022). Scattering and
1574 Absorbing Aerosols in the Climate System. *Nature Rev. Earth Env.*, doi:10.1038/s43017-022-
1575 00296-7.
1576
1577 Lim, H., Choi, M., Kim, J., Kasai, Y.,& Chan, P.W. (2018). AHI/Himawari-8 Yonsei Aerosol
1578 Retrieval (YAER): Algorithm, validation and merged products. *Remote Sens., 10, 699*,
1579 doi:10.3390/rs10050699.
1580
1581 Liu, X., Penner, J.E., Ghan, S.J., & Wang, M. (2007). Inclusion of ice microphysics in the
1582 NCAR Community Atmospheric Model Version 3 (CAM3). *J. Climate 20, 4526-4547*.
1583
1584 Loeb, N.G., & Su, W. (2010). Direct aerosol radiative forcing uncertainty based on a radiative
1585 perturbation analysis. *J. Climate 23, 5288–5293*, doi:10.1175/2010JCLI3543.1.
1586
1587 Lu, Z., Wang, J., Xu, X., Chen, X., Kondragunta, S., Torres, O., et al. (2021). Hourly mapping of
1588 the layer height of thick smoke plumes over the western U.S. in 2020 severe fire season. *Front.*
1589 *Remote Sens. 2, 766628*, doi:10.3389/frsen.2021.766628.
1590

1591 Lyapustin, A., Wang, Y., Korkin, S., Kahn, R.A., & Winker, D. (2020). MAIAC thermal
1592 technique for smoke injection height from MODIS. *IEEE Geosci. Remt. Sens. Lett. 17 (5), 730-*
1593 *734*, doi: 10.1109/LGRS.2019.2936332.
1594
1595 Lyapustin, A., Go, S., Korkin, S., Wang, Y., Torres, O., et al. (2021). Retrievals of Aerosol
1596 Optical Depth and Spectral Absorption From DSCOVR EPIC. *Front. Remt. Sens. 2, 645794*,
1597 doi:10.3389/frsen.2021.645794.
1598
1599 Malm, W.C, & Hand, J.L. (2007). An examination of the physical and optical properties of
1600 aerosols collected in the IMPROVE program. *Atmos. Env. 41, 3407–3427*,
1601 doi:10.1016/j.atmosenv.2006.12.012.
1602
1603 Mann, G.W., Carslaw, K.S., Spracklen, D.V., Ridley, D.A., Manktelow, P.T., Chipperfield,
1604 M.P., et al. (2010). Description and evaluation of GLOMAP-mode: a modal global
1605 aerosol microphysics model for the UKCA composition-climate model. *Geosci. Model Dev., 3*,
1606 *519–551*, doi:10.5194/gmd-3-519-2010.
1607
1608 Marinescu, P.J., van den Heever, S.C., Heikenfeld, M., Barrett, A.I., Barthlott, C., Hoose, C., et
1609 al. (2021). Impacts of Varying Concentrations of Cloud Condensation Nuclei on Deep
1610 Convective Cloud Updrafts – A Multimodel Assessment. *J. Atmosph. Sci. 78, 1147-1172*,
1611 doi:10.1175/JAS-D-20-0200.1.
1612
1613 Marshak, A., Herman, J., Szabo, A., Blank, K., Carn, S., Cede, A., et al. (2018). Earth
1614 Observations from DSCOVR/EPIC Instrument. *Bulletin Amer. Meteor. Soc. (BAMS), 9, 1829-*
1615 *1850*, doi:10.1175/BAMS-D-17-0223.1.
1616
1617 Marshak, A., Ackerman, A., Da Silva, A., Eck, T., Holben, B.N., Kahn, R.A., et al. (2021).
1618 Aerosol properties in cloudy environments from remote sensing observations: review of current
1619 state of knowledge. *Bull. Am. Meteorol. Soc. E2177-E2197*, doi:10.1175/BAMS-D-20-0225.1.
1620

1621 Martin, S.T., Artaxo, P., Machado, L., Manzi, A.O., Souza, R.R.F., et al. (2017). The Green
1622 Ocean AMAZON experiment (GOAMAZON 2014/2015) observes pollution affecting gases,
1623 aerosols, couds, and rainfall of the rain forest. *Bulletin Amer. Meteor. Soc. (BAMS), 981-997,*
1624 doi: 10.1175/BAMS-D-15-00221.1.
1625
1626 Martins, J.V. (2016). Airborne Open Polar/Imaging Nephelometer for Ice Particles in Cirrus
1627 Clouds and Aerosols Field Campaign Report. *U.S. Dept. of Energy, Office of Science, ARM*
1628 *Climate Research Facility, DOE/SC-ARM-15-063*.
1629
1630 Mather, J. H., & Voyles, J. W. (2013). The ARM Climate Research Facility: A review of
1631 structure and capabilities, *Bull. Am. Meteorol. Soc.*, *94*(3)*, 377-392*. doi:10.1175/BAMS-D-11-
1632 00218.1.
1633
1634 McCoy, D.T., Tan, I., Hartmann, D.L., Zelinka, M.D., Storelvmo, T. (2016). On the relationships
1635 among cloud cover, mixed-phase partitioning, and planetary albedo in GCMs. *J. Adv. Model.*
1636 *Earth Syst., 8*, doi:10.1002/2015MS000589.
1637
1638 McFiggans, G., Artaxo, P., Baltensperger, U., Coe, H., Facchini, M.C., Feingold, G., et al.
1639 (2006). The effect of physical and chemical aerosol properties on warm cloud droplet activation.
1640 *Atmos. Chem. Phys., 6, 2593–2649*, doi:10.5194/acp-6-2593-2006.
1641
1642 Mechoso, C.R., Wood, R., Weller, R., Bretherton, C.S., Clarke, A.D., et al. (2014). Ocean-
1643 Cloud-Atmosphere-Land interactions in the southeastern Pacific: The VOCALS program. *Bull.*
1644 *Am. Meteoro. Soc. 95, 357-375*, doi: 10.1175/BAMS-D-11-00246.1.
1645
1646 Meyer, K., Platnick, S., & Zhang, Z. (2015). Simultaneously inferring above-cloud absorbing
1647 aerosol optical thickness and underlying liquid phase cloud optical and microphysical properties
1648 using MODIS. *J. Geophys. Res. Atm. 120, 5524-5547*, doi:10.1002/2015JD023128
1649

McComiskey A., Schwartz, S.E., Schmid, B., Guan, H., Lewis, E.R., Ricchiazzi, P., & Ogren, J.A. (2008). Direct aerosol forcing: calculation from observables and sensitivities to inputs. *J. Geophys. Res. 113, D09202*, doi:10.1029/2007JD009170.

McNeill, J., Snyder, G., Weagle, C.L., Walsh, B., Bissonnette, P., Stone, E., et al. (2020). Large global variations in measured airborne metal concentrations driven by anthropogenic sources. *Nature Sci. Rep. 10:21817*, doi:10.1038/s41598-020-78789-y.

Menon, S., Hansen, J., Nazarenko, L., and Y. Luo, Y. (2002), Climate effects of black carbon aerosols in China and India. *Science, 297, 2250–2253*, doi: 10.1126/science.1075159.

Mishchenko, M.I., & Travis, L.D. (1997). Satellite retrieval of aerosol properties over the ocean using polarization as well as intensity of reflected sunlight. *J. Geophys. Res. 102 (D14) 16,989-17,013,* doi:10.1029/96JD02425.

Morales Betancourt, R., & Nenes, A. (2014). Understanding the contributions of aerosol properties and parameterization discrepancies to droplet number variability in a global climate model. *Atmos. Chem. Phys., 14, 4809–4826*, doi: 10.5194/acp-14-4809-2014.

Mortier, A., Gliss, J., Schulz, M., Aas, W., Andrews, E., Bian, H., et al. (2020). Evaluation of climate model aerosol trends with ground-based observations over the last two decades – an AeroCom and CMIP6 analysis. *Atmos. Chem. Phys., 20, 13355–13378*. doi:10.5194/acp-20-13355-2020.

Mülmenstädt, J. & Feingold, G. (2018). The radiative forcing of aerosol-cloud interactions in liquid clouds: Wrestling and embracing uncertainty. *Curr. Clim. Change Rep., 4, 23–40*, doi:10.1007/s40641-018-0089-y, 2018.

Myhre, G., Samset, B.H., Schulz, M., Balkanski, Y., Bauer, S., Berntsen, T.K., et al. (2013). Radiative forcing of the direct aerosol effect from AeroCom Phase II simulations. *Atmos. Chem. Phys. 13, 1853–1877,* doi:10.5194/acp-13-1853-2013.

Nakajima, T., Higurashi, A., Kawamoto, K., & Penner, J.E. (2001). A possible correlation between satellite-derived cloud and aerosol microphysical parameters. *Geophys. Res. Lett. 28 (7), 1171-1174,* doi:10.1029/2000GL012186.

Nazarenko, L., Rind, D., Tsigaridis, K., Del Genio, A.D., Kelley, M., & Tausnev, N. (2017). Interactive nature of climate change and aerosol forcing. *J. Geophys. Res. Atmos., 122, 3457–3480*, doi:10.1002/2016JD025809.

Nelson, D.L., Garay, M.J., Kahn, R.A., & Dunst, B.A. (2013). Stereoscopic height and wind retrievals for aerosol plumes with the MISR INteractive eXplorer (MINX). *Remote Sens. 5*, *4593-4628*, doi:10.3390/rs5094593.

Nguyen, H.N., Gudmundsson, A., & Martinsson, B.G. (2006). Design and calibration of a multi-channel aerosol sampler for tropopause region studies from the CARIBIC platform. *Aerosol Sci. Tech., 40:649–655*, doi:10.1080/02786820600767807.

Nicolae, D., Vasilescu, J., Talianu, C., Binietoglou, I., Nicolae, V., Andrei, S., & Antonescu, B. (2018). A neural network aerosol-typing algorithm based on lidar data. *Atmos. Chem. Phys., 18, 14511–14537*, doi:10.5194/acp-18-14511-2018.

O'Gorman, P.A., Allan, R.P., Byrne, M.P., & Previdi, M. (2012). Energetic constraints on precipitation under climate change. *Survy. Geophys. 33, 585-608*, doi:10.1007/s10712-011-9159-6.

Pahlow, M., Feingold, G., Jefferson, A., Andrews, E., Ogren, J.A., Wang, J., et al. (2006). Comparison between lidar and nephelometer measurements of aerosol hygroscopicity at the Southern Great Plains Atmospheric Radiation Measurement site. *J. Geophys. Res., 111, D05S15*, doi:10.1029/2004JD005646.

1711 Pan, X., Chin, M., Gautam, R., Bian, H., Kim, D., Colarco, P.R., et al. (2015). A multi-model
1712 evaluation of aerosols over South Asia: Common problems and possible causes. *Atmos. Chem.*
1713 *Phys. 15, 5903-5928*, doi:10.5194/acp-15-5903-2015.
1714
1715 Papagiannopoulos, N., Mona, L., Amodeo, A., D'Amico, G., Gumà Claramunt, P., Pappalardo,
1716 G., et al. (2018). An automatic observation-based aerosol typing method for EARLINET. *Atmos.*
1717 *Chem. Phys., 18, 15879–15901*, doi:10.5194/acp-18-15879-2018.
1718
1719 Pappalardo, G., Amodeo, A., Apituley, A., Comeron, A., Freudenthaler, V., Linn, H.,et al.
1720 (2014). EARLINET: towards an advanced sustainable European aerosol lidar network. *Atmos.*
1721 *Meas. Tech., 7, 2389–2409*, doi:10.5194/amt-7-2389-2014.
1722
1723 Persad, G.G., Samset, B.H., & Laura J. Wilcox, L.J. (2022). Aerosols must be included in
1724 climate risk assessments, *Nature, 611 (24), 662-664*. doi:10.1038/d41586-022-03763-9.
1725
1726 Petrenko, M., Kahn, R.A., Chin, M., & Limbacher, J.A. (2017). Refined use of satellite aerosol
1727 optical depth snapshots to constrain biomass burning emissions in the GOCART model. *J.*
1728 *Geophys. Res. 122,* doi:10.1002/2017JD026693.
1729
1730 Pu, B., Ginoux, P., Guo, H., Hsu, C., Kimball, J., et al. (2020). Retrieving the global distribution
1731 of the threshold of wind erosion from satellite data and implementing it into the Geophysical
1732 Fluid Dynamics Laboratory land–atmosphere model (GFDL AM4.0/LM4.0). *Atmos. Chem.*
1733 *Phys., 20, 55–81*, doi:10.5194/acp-20-55-2020.
1734
1735 Quaas, J., Arola, A., Cairns, B., Christensen, M., Deneke, H., Ekman, A.M.L., et al. (2020).
1736 Constraining the Twomey effect from satellite observations: Issues and perspectives. *Atmos.*
1737 *Chem. Phys., 20, 15079–15099*, doi:10.5194/acp-20-15079-2020.
1738
1739 Quaas, J., Hailing, J., Smith, C., Albright, A.L., Aas, W., Bellouin, N., et al. (2022). Robust
1740 evidence for reversal of the trend in aerosol effective climate forcing. *Atmos. Chem. Phys., 22,*
1741 *12221–12239*, doi: 10.5194/acp-22-12221-2022.

Ramaswamy, V., Boucher, O., Haigh, J., Hauglustaine, D., Haywood, J., et al. (2001). Ch. 6, Radiative forcing of climate change. In: Climate Change 2001: The Scientific Basis, J. T. Houghton et al., Eds., Cambridge University Press, 349–416.

Randerson, J. T., Chen, Y., van der Werf, G. R., & Morton, D. C. (2012). Global burned area and biomass burning emissions from small fires. *J. Geophys. Res. 117, G04012*, doi:10.1029/2012JG002128.

Randles, C. A., da Silva, A.M., Buchard, V., Colarco, P.R., Darmenov, A., Govindaraju, R.,et al. (2017). The MERRA-2 aerosol reanalysis, 1980–onward, Part I: System description and data assimilation evaluation. *J. Climate 30, 6823-6850*, doi:10.1175/jcli-d-16-0609.s1.

Reddington, C.L., Carslaw, K.S., Stier, P., Schutgens, N., Coe, H., Liu, D., et al. (2017). The global aerosol synthesis and science project (GASSP). *Bull. Am. Meteoro. Soc. 1857-1877*, doi:10.1175/BAMS-D-15-00317.1.

Redemann, J., Wood, R., Zuidema, P., Doherty, S.J., Luna, B., LeBlanc, S.E., et al. (2021). An overview of the ORACLES (ObseRvations of Aerosols above CLouds and their intEractionS) project: aerosol–cloud–radiation interactions in the southeast Atlantic basin. *Atmos. Chem. Phys., 21, 1507–1563*, doi:10.5194/acp-21-1507-2021.

Reid, J.S., R. Koppmann, R., Eck, T.F., & Eleuterio, D.P. (2005). A review of biomass burning emissions part II: intensive physical properties of biomass burning particles. *Atmos. Chem. Phys., 5, 799–825*, doi:1680-7324/acp/2005-5-799.

Reid, J.S., Reid, E.A., Walker, A., Piketh, S., Cliff, S., Al Mandoos, A., et al. (2008). Dynamics of southwest Asian dust particle size characteristics with implications for global dust research. *J. Geophys. Res., 113, D14212*, doi:10.1029/2007JD009752.

1772 Reid, J.S., Hyer, E.J., Prins, E.M., Westphal, D.L., Zhang, J., et al. (2009). Global monitoring
1773 and forecasting of biomass-burning smoke: Description of and lessons from the Fire Locating
1774 and Modeling of Burning Emissions (FLAMBE) program. *IEEE J. Topics Applied Earth Obs. &*
1775 *Remt. Sens. 2 (3), 144-162*, doi:1939-1404/26.00.
1776
1777 Remer, L.A., Kaufman, Y.J., Tanre, D., Mattoo, S., Chu, D.A., Martins, J.V., et al. (2005). The
1778 MODIS aerosol algorithm, products, and validation. *J. Atmos. Sci., 62, 947–973*,
1779 doi:10.1175/JAS3385.1.
1780
1781 Reutter, P., Su, H., Trentmann, J., Simmel, M., Rose, D., Gunthe, S. S., Wernli, H., et al. (2009).
1782 Aerosol- and updraft-limited regimes of cloud droplet formation: influence of particle number,
1783 size and hygroscopicity on the activation of cloud condensation nuclei (CCN), *Atmos. Chem.*
1784 *Phys., 9, 7067–7080*, doi:10.5194/acp-9-7067-2009.
1785
1786 Rissman, T., Nenes, A., & Seinfeld, J.H. (2004). Chemical amplification (or dampening) of the
1787 Twomey effect: Conditions derived from droplet activation theory. *J. Atmos. Sci., 61(8), 919-*
1788 *930*, doi:10.1175/1520-0469.
1789
1790 Rose, C., Coen, M.C., Andrews, E., Lin, Y., Bossert, I., Myhre, C.L., et al. (2021). Seasonality of
1791 the particle number concentration and size distribution: a global analysis retrieved from the
1792 network of Global Atmosphere Watch (GAW) near-surface observatories. *Atmos. Chem. Phys.,*
1793 *21, 17185–17223*, doi:10.5194/acp-21-17185-2021.
1794
1795 Rosenfeld, D., Andreae, M.O., Asmi, A., Mian Chin, M., de Leeuw, G., Donovan, D.P., et al.
1796 (2014). Global observations of aerosol-cloud-precipitation-climate. *Rev. Geophys*. *52,*
1797 doi:10.1002/2013RG000441.
1798
1799 Rosenfeld, D., Zheng, Y., Hashimshoni, E., Pöhlker, M.L., Jeferson, A., Pöhlker, C., et al.
1800 (2016). Satellite retrieval of cloud condensation nuclei concentrations by using clouds as CCN
1801 chambers. *Proc. Nat. Acad. Sci. 113 (21)*, doi:10.1073/pnas.1514044113.
1802

1803 Rubin, J.I., Reid, J.S., Hansen, J.A., Anderson, J.L., Holben, B.N., Xian, P., et al. (2017).
1804 Assimilation of AERONET and MODIS AOT observations using variational and ensemble data
1805 assimilation methods and its impact on aerosol forecasting skill. *J. Geophys. Res. Atmos. 122,*
1806 *4967–4992*. doi:10.1002/2016JD026067.
1807
1808 Russell, P.B., Kacenelenbogen, M., Livingston, J.M., Hasekamp, O.P., Burton, S.P., Schuster,
1809 G.L., et al. (2014). A multiparameter aerosol classification method and its application to
1810 retrievals from spaceborne polarimetry. *J. Geophys. Res. Atmos. 119*,
1811 doi:10.1002/2013JD021411.
1812
1813 Samset, B. H., G. Myhre, M. Schulz, Balkanski, Y., Bauer, S., Berntsen, T.K., et al. (2013).
1814 Black carbon vertical profiles strongly affect its radiative forcing uncertainty. *Atmos. Chem.*
1815 *Phys. 13(5), 2423–2434*, doi:10.5194/acp-13-2423-2013.
1816
1817 Samset, B., Myhre, G. & Schulz, M. (2014). Upward adjustment needed for aerosol radiative
1818 forcing uncertainty. *Nature Climate Change 4, 230–232*. doi:10.1038/nclimate2170.
1819
1820 Sand, M., Samset, B.H., Balkanski, Y., Bauer, S., Bellouin, N., Berntsen, T.K., et al. (2017).
1821 Aerosols at the poles: an AeroCom Phase II multi-model evaluation. *Atmos. Chem. Phys. 17,*
1822 *12197–12218*. doi:10.5194/acp-17-12197-2017.
1823
1824 Sayer, A.M., Hsu, N.C., Lee, J., Kim, W.V., Burton, S., Fenn, M.A., et al. (2019). Two decades
1825 observing smoke above clouds in the south-eastern Atlantic Ocean: Deep Blue algorithm updates
1826 and validation with ORACLES field campaign data. *Atmos. Meas. Tech., 12, 3595–3627*,
1827 doi:10.5194/amt-12-3595-2019.
1828
1829 Sayer, A.M., Govaerts, Y., Kolmonen, P., Lipponen, A., Luffarelli, M., Mielonen, T., et al.
1830 (2020). A review and framework for the evaluation of pixel-level uncertainty estimates in
1831 satellite aerosol remote sensing. *Atmos. Meas. Tech. 13, 373–404*, doi:10.5194/amt-13-373-2020.
1832

Schill, G.P., Froyd, K.D., Bian, H., Kupc, A., Williamson, C., Brock, C.A., et al. (2020). Widespread biomass burning smoke throughout the remote troposphere. *Nature Geosci.*, doi:10.1038/s41561-020-0586-1.

Schroeder, P., Brewer, W.A., Choukulkar, A., Weickmann, A., Zucker, M, Holloway, M.W., & Sandberg, S. 2020. A compact, flexible, and robust micropulsed Doppler lidar. *J. Atmosph. Ocean Tech. 37, 1387-1402*, doi:10.1175/JTECH-D-19-0142.1.

Schulz, M., Textor, C., Kinne, S., Balkanski, Y., Bauer, S., Berntsen, T., et al. (2006). Radiative forcing by aerosols as derived from the AeroCom present-day and pre-industrial simulations. *Atmos. Chem. Phys. 6(12), 5225–5246,* doi:10.5194/acp-6-5225-2006.

Schuster, G.L., & Trepte, C. (2021). Models, In situ, and Remote sensing of Aerosols (MIRA). https://science.larc.nasa.gov/wpcontent/uploads/sites/147/2021/11/MIRA_newsletter_20211027.pdf (last accessed 05/02/2022)

Schutgens, N., Tsyro, S., Gruspeerdt. E., Goto, D., Weigum, N.,, Schultz, M., & Stier, P. (2017). On the spatio-temporal representativeness of observations. *Atmos. Chem. Phys., 17, 9761-8780*, doi:10.5194/acp-17-9761-2017.

Schutgens, N., Sayer, A.M., Heckel, A., Hsu, N.C., Jethva, H., de Leeuw, G., et al. (2020). An AeroCom–AeroSat study: intercomparison of satellite AOD datasets for aerosol model evaluation. *Atmos. Chem. Phys. 20, 12431–12457*, doi:10.5194/acp-20-12431-2020.

Schutgens, N., Dubovik, O., Hasekamp, O., Torres, O., Jethva, H.,Leonard, P.J.T., et al. (2021). AEROCOM and AEROSAT AAOD and SSA study – Part 1: Evaluation and intercomparison of satellite measurements. *Atmos. Chem. Phys., 21, 6895–6917*, doi:10.5194/acp-21-6895-2021.

Seidel, F., & C. Popp (2012). Critical surface albedo and its implications to aerosol remote sensing. Atmos. Meas. Tech., 5, 1653–1665, doi: 10.5194/amt-5-1653-2012.

1864 Seinfeld, J.H., Bretherton, C.S., Carslaw, K.S., Coe, H., DeMott, P.J., Dunlea, E.J., et al. (2016).
1865 Improving our fundamental understanding of the role of aerosol-cloud interactions in the climate
1866 system. *Proc. Nat. Academy Sci*. *113 (21),* 5781–5790, doi:10.1073/pnas.1514043113.
1867
1868 Sekiyama, T. T., Tanaka, T. Y., Shimizu, A., & Miyoshi, T. (2010). Data assimilation of
1869 CALIPSO aerosol observations. *Atmos. Chem. Phys., 10, 39–49*. doi:10.5194/acp-10-39-2010.
1870
1871 Shen, Y., Virkkula, A., Ding, A., Luoma, K., Keskinen, H., Aalto, P. P., et al. (2019). Estimating
1872 cloud condensation nuclei number concentrations using aerosol optical properties: role of
1873 particle number size distribution and parameterization, *Atmos. Chem. Phys., 19, 15483–15502*,
1874 doi:10.5194/acp-19-15483-2019.
1875
1876 Sheridan, J.P., Andrews, E., Ogren, J.A., Tackett, J.L., & Winker, D.M., (2012). Vertical profiles
1877 of aerosol optical properties over Central Illinois and comparison with surface and satellite
1878 measurements. *Atmos. Chem. Phys., 12, 11695–11721*, doi:10.5194/acp-12-11695-2012.
1879
1880 Shindell, D.T., Lamarque, J.-F., Schulz, M., Flanner, M., Jiao, C., Chin, M., et al. (2013).
1881 Radiative forcing in the ACCMIP historical and future climate simulations. *Atmos. Chem. Phys.,*
1882 *13, 2939–2974*, doi: 10.5194/acp-13-2939-2013.
1883
1884 Shinozuka, Y., Clarke, A.D., Nenes, A., Jefferson, A., Wood, R., McNaughton, C.S., et al.
1885 (2015). The relationship between cloud condensation nuclei (CCN) concentration and light
1886 extinction of dried particles: indications of underlying aerosol processes and implications for
1887 satellite-based CCN estimates. *Atmos. Chem. Phys., 15, 7585-7604*, doi:10.5194/acp-15-7585-
1888 2015.
1889
1890 Smirnov, A, Holben, B.N., Giles, D.M., Slutsker, I., O'Neill, N.T., Eck, T.F., et al. (2011).
1891 Maritime aerosol network as a component of AERONET – First results and comparison with
1892 global aerosol models and satellite retrievals. *Atmos. Meas. Tech. 4*, 583-597, doi:10.5194/amt-4-
1893 583-2011.
1894

1895 Snider, G., Weagle, C.L., Martin, R.V., van Donkelaar, A., Conrad; K., Zwicker, M., et al.
1896 (2015). SPARTAN: A global network to evaluate and enhance satellite-based estimates of
1897 ground-level aerosol for global health applications. *Atmos. Meas. Tech. 8, 505-521*,
1898 doi:10.5194/amt-8-505-2015.
1899
1900 Soden, B., and Chung, E.-S. (2017). The Large-Scale Dynamical Response of Clouds to Aerosol
1901 Forcing. *J Clim. 30(21), 8783–8794*, doi:10.1175/JCLI-D-17-0050.1.
1902
1903 Sogacheva, L., Popp, T., Sayer, A. M., Dubovik, O., Garay, M. J., Heckel, A., et al. (2020).
1904 Merging regional and global aerosol optical depth records from major available satellite
1905 products, *Atmos. Chem. Phys., 20, 2031–2056*, https://doi.org/10.5194/acp-20-2031-2020.
1906
1907 Sorooshian, A., Anderson, B., Bauer, S.E., Braun, R.A., Cairns, B., et al. (2019), Aerosol-Cloud-
1908 Meteorology interaction airborne field investigations: Using Lessons Learned from the U.S.
1909 West Coast in the Design of ACTIVATE off the U.S. East Coast. *Bull. Am. Meteor. Soc. 100,*
1910 *1511–1528*, doi:10.1175/BAMS-D-18-0100.1.
1911
1912 Sorooshian, A., Atkinson, J., Ferrare, R., Hair, J., & Ziemba, L. (2021). Taking flight to study
1913 clouds and climate. *Eos,102,* doi:10.1029/2021EO158570.
1914
1915 Stier, P., Feichter, J., Kinne, S., Kloster, S., Vignati, E., Wilson, J., et al. (2005). The aerosol-
1916 climate model ECHAM5-HAM. *Atmos. Chem. Phys., 5, 1125–1156*, doi: 10.5194/acp-5-1125-
1917 2005.
1918
1919 Stier, P., Schutgens, N.A.J., Bellouin, N., Bian, H., Boucher, O., Chin, M., et al. (2013). Host
1920 model uncertainties in aerosol radiative forcing estimates: results from the AeroCom Prescribed
1921 intercomparison study. *Atmos. Chem. Phys., 13, 3245–3270*, doi: 10.5194/acp-13-3245-2013.
1922
1923 Stier, P. (2016). Limitations of passive remote sensing to constrain global cloud condensation
1924 nuclei. *Atmos. Chem. Phys., 16, 6595–6607*, doi:10.5194/acp-16-6595-2016.
1925

1926 Sullivan, S.C., Lee, D., Oreopoulos, L., & Nenes, A. (2016). Role of updraft velocity in temporal
1927 variability of global cloud hydrometeor number. *Proc. Nat. Acad. Sci. 113 (21), 5791-5796*,
1928 doi:10.1073/pnas.1514039113.
1929
1930 Tao, W.-K., Chen, J.-P., Li, Z., Wang, C., & Zhang, C. (2012). Impact of aerosols on convective
1931 clouds and precipitation. *Rev. Geophys., 50, RG2001*, doi:10.1029/2011RG000369.
1932
1933 Textor, C., Schulz, M., Guibert, S., Kinne, S., Balkanski, Y., Bauer, S., et al. (2006). Analysis
1934 and quantification of the diversities of aerosol life cycles within AeroCom, *Atmos. Chem. Phys.,*
1935 *6*, 1777–1813.
1936
1937 Textor, C., Schulz, M., Guibert, S., Kinne, S., Balkanski, Y., Bauer, S., et al. (2007). The effect
1938 of harmonized emissions on aerosol properties in global models – an AeroCom experiment.
1939 *Atmos. Chem. Phys., 7, 4489–4501*, doi:10.5194/acp-7-4489-2007.
1940
1941 Thomas, G.E., Poulsen, C.A., Sayer, A.M., Marsh, S.H., Dean, S.M., Carboni, E., et al. (2009).
1942 The GRAPE aerosol retrieval algorithm. *Atmos. Meas. Tech., 2, 679–701*, doi:10.5194/amt-2-
1943 679-2009.
1944
1945 Thorsen, T.J., Winker, D.M., & Ferrare, R.A. (2021). Uncertainty in observational estimates of
1946 the aerosol direct radiative effect and forcing. *J. Climate 34, 195-213*, doi:10.1175/JCLI-D-19-
1947 1009.1.
1948
1949 Tsigaridis, K., Daskalakis, N., Kanakidou, M., Adams, P. J., Artaxo, P., Bahadur, R., et al.
1950 (2014). The AeroCom evaluation and intercomparison of organic aerosol in global models.
1951 *Atmos. Chem. Phys., 14, 10845–10895*, doi:10.5194/acp-14-10845-2014.
1952
1953 Toon, O. B., Maring, H., Dibb, J., Ferrare, R., Jacob, D.J., Jensen, E.J., et al. (2016). Planning,
1954 implementation, and scientific goals of the Studies of Emissions and Atmospheric Composition,
1955 Clouds and Climate Coupling by Regional Surveys (SEAC4RS) field mission. *J. Geophys. Res.*
1956 *Atmos., 121,* doi:10.1002/2015JD024297.

Torres, O., Jethva, H., & Bhartia, P.K. (2012). Retrieval of aerosol optical depth above clouds from OMI observations: sensitivity analysis and case studies. *J. Atmos. Sci. 69, 1037–1053*, doi:10.1175/JASD-11-0130.1.

Twomey, S. (1974). Pollution and the planetary albedo. *Atmos. Env. 8, 1251-1256*, doi: 10.1016/0004-6981(74)90004-3.

Twomey, S. (1977). The influence of pollution on the short wave albedo of clouds. *J. Atmos. Sci., 34, 1149–1152*, doi:10.1175/1520-0469(1977)034.

Val Martin, M. Kahn, R.A., & Tosca, M. (2018). A global climatology of wildfire smoke injection height derived from space-based multi-angle imaging. *Remote Sensing 10, 1609*, doi:10.3390/rs10101609.

Vandenbussche, S., Kochenova, S., Vandaele, A.C., Kumps, N., & De Maziere, M. (2013). Retrieval of desert dust aerosol vertical profiles from IASI measurements in the TIR atmospheric window. *Atmos. Meas. Tech., 6, 2577–2591*, doi:10.5194/amt-6-2577-2013.

van der Werf, G.R., Randerson, J.T., Giglio, L., van Leeuwen, T.T., Chen, Y., et al. (2017). Global fire emissions estimates during 1997–2016. *Earth Syst. Sci. Data, 9, 697–720*, doi: 10.5194/essd-9-697-2017.

Van Donkelaar, A., Martin, R.V., Brauer, M., Kahn, R.A., Levy, R.C., Verduzco, C., & Villeneuve, P. (2010). Global estimates of average ground-level fine particulate matter concentrations from satellite-based aerosol optical depth. *Environ. Health Perspect. 118, 847-855*, doi:10.1289/EHP.0901623.

Van Donkelaar, A., M. Hammer, M., Bindle, L., Brauer, M., Brook, J., Garay, M., et al. (2021). Monthly global estimates of fine particulate matter and their uncertainty. *Environ. Sci. Tech. 55, 15287−15300*, doi:10.1021/acs.est.1c05309.

Vernon, C.J., Bolt, R., Canty, T., & Kahn, R.A. (2018). The impact of MISR-derived injection-height initialization on wildfire and volcanic plume dispersion in the HySPLIT model. *Atmos. Meas. Tech*. *11*, *6289–6307*, doi:10.5194/amt-11-6289-2018.

Vicent, J., Verrelst, J., Sabater, N., Alonso, L., Rivera-Caicedo, J.P., Martino, L., et al. (2020). Comparative analysis of atmospheric radiative transfer models using the Atmospheric Look-up table Generator (ALG) toolbox (version 2.0). *Geosci. Model Dev., 13, 1945–1957*, doi:10.5194/gmd-13-1945-2020.

Vogelmann, A., G. M. McFarquhar, J. A. Ogren, D. D. Turner, J. M. Comstock, G. Feingold, et al. (2012). RACORO extended-term, aircraft observations of boundary-layer clouds, *Bull. Amer. Meteor. Soc., 93, 861-878*, doi:10.1175/BAMS-D-11-00189.1.

Wang, J., Aegerter, C., Xu, X., & Szykman, J.J. (2016). Potential application of VIIRS Day/Night Band for monitoring nighttime surface PM2.5 air quality from space. *Atmosph. Environ. 124, 55-63*, doi:10.1016/j.atmosenv.2015.11.013.

Wang, S., Wang Q., & Feingold, G. (2003). Turbulence, condensation, and liquid water transport in numerically simulated nonprecipitating stratocumulus clouds. *J. Atmos. Sci., 60, 262–278*, doi:10.1175/1520-0469.

Watson-Parris, D., Schutgens, N., Reddington, C., Pringle, K.J., Liu, D., et al. (2019). In situ constraints on the vertical distribution of global aerosol. *Atmos. Chem. Phys., 19, 11765–11790*, doi:10.5194/acp-19-11765-2019.

Watson-Parris, D., & Smith, C.J. (2022). Large uncertainty in future warming due to aerosol forcing. *Nat. Clim. Chang. 12, 1111–1113*, doi:10.1038/s41558-022-01516-0.

2017 Wells, K.C., Martins, J.V., Remer, L.A., Kreidenweis, S.M., & G. L. Stephens G.L. (2012).
2018 Critical reflectance derived from MODIS: Application for the retrieval of aerosol absorption over
2019 desert regions, *J. Geophys. Res., 117, D03202*, doi:10.1029/2011JD016891.
2020
2021 Welton, E.J., Campbell, J.R., Spinhirne, J.D., & Scott, V.S. (2001). Global monitoring of clouds
2022 and aerosols using a network of micro-pulse lidar systems. *Proc. SPIE 4153, 151-158,*
2023 doi:10.1117/12.417040.
2024
2025 Wen, G., Marshak, A.,Cahalan, R.F., Remer, L., & Kleidman, R.G. (2007). 3D aerosol-cloud
2026 radiative interaction observed in collocated MODIS and ASTER images of cumulus cloud fields.
2027 *J. Geophys. Res., 112, D13204*, doi:10.1029/2006JD008267.
2028
2029 Werdell, P.J., Behrenfeld, M.J., Bontempi, P.S., Boss, E., Caorms. B. et al. (2019). The plankton,
2030 aerosol, cloud, ocean ecosystem mission: Status, science, advances. *Bull. Am. Meteorol. Soc.*
2031 *1775-1794*, doi:10.1175/BAMS-D-18-0056.1.
2032
2033 Wiggins, E.B., Soja, A.J., Gargulinski, E., Halliday, H.S., Pierce, R.B., et al. (2020). High
2034 Temporal Resolution Satellite Observations of Fire Radiative Power Reveal Link Between Fire
2035 Behavior and Aerosol and Gas Emissions. *Geophys. Res. Lett. 47, e2020GL090707*,
2036 doi:10.1029/2020GL090707
2037
2038 Williams, A.I.L., Stier, P., Dagan, G., & Watson-Parris, D. (2022). Strong control of effective
2039 radiative forcing by the spatial pattern of absorbing aerosol. *Nature Climate Change (12), 735-*
2040 *742*, doi:10.1038/s41558-022-01415-4.
2041
2042 Wilson, J.C., Lafleu, B.G., Hilbert, H., Seebaugh, W.R., Fox, J., Gesler, D.W., Brock, C.A.,
2043 Huebert, B.J., & Mullen, J. (2004) Function and performance of a low turbulence inlet for
2044 sampling supermicron particles from aircraft platforms. *Aerosol Sci. Tech., 38(8), 790-802*,
2045 doi:10.1080/027868290500841.
2046

2047 Winker, D.M., Vaughan, M.A., Omar, A., Hu, Y., & Powell, K.A. (2009). Overview of the
2048 CALIPSO mission and CALIOP data processing algorithms. *J. Atmos. Ocean Technol. 26,*
2049 *2310–2323*, doi:10.1175/2009JTECHA1281.1.
2050
2051 Witek, M.L., Garay, M.J., Diner, D.J., Bull, M.A., & Seidel, F.C. (2018). New approach to the
2052 retrieval of AOD and its uncertainty from MISR observations over dark water. *Atmos. Meas.*
2053 *Tech. 11, 429–439*, doi:10.5194/amt-11-429-2018.
2054
2055 Xian, P., Reid, J.S., Hyer, E.J., Sampson, C.R., Rubin, J.I., Ades, M. et al. (2019). Current state
2056 of the global operational aerosol multi-model ensemble: An update from the International
2057 Cooperative for Aerosol Prediction (ICAP). *Q. J. Royal Meteoro. Soc. 145 (Suppl.), 176–209*,
2058 doi:10.1002/qj.3497.
2059
2060 Xue, H., Feingold, G., & Stevens, B. 2008. Aerosol effects on clouds, precipitation, and the
2061 organization of shallow cumulus convection. *J. Atmos. Sci., 65, 392–406*,
2062 doi:10.1175/2007JAS2428.1.
2063
2064 Yang, C.K., Chiu, J.C., Marchak, A., Feingold, G., Varnai, T., Wen, G., et al. (2022). Near-cloud
2065 aerosol retrieval Uusing machine learning techniques, and implied direct radiative effects.
2066 *Geophys. Res. Lett. 49, e2022GL098274*, doi:10.1029/2022GL098274.
2067
2068 Yokelson, R., Crounse, J. D., DeCarlo, P. F., Karl, T., Urbanski, S., Atlas, E., et al. (2009).
2069 Emissions from biomass burning in the Yucatan. *Atmos. Chem. Phys., 9, 5785-5812,*
2070 doi:10.5194/acp-9-5785-2009.
2071
2072 Yorks, J.E., McGill, M.J., Palm, S.P., Hlavka, D.L., Selmer, P.A., Nowottnick, E.P., et al.
2073 (2016). An overview of the CATS level 1 processing algorithms and data products. *Geophys.*
2074 *Res. Lett., 43, 4632–4639*, doi:10.1002/2016GL068006.
2075

2076 Zamora, L.M., & Kahn, R.A. (2020). Saharan dust aerosols change deep convective cloud
2077 prevalence, possibly by inhibiting marine new particle formation. *J. Climate 33, 9467-9477*,
2078 doi:10.1175/JCLI-D-20-0083.1
2079
2080 Zender, C.S., Bian, H., & Newman, D. (2003). Mineral Dust Entrainment and Deposition
2081 (DEAD) model: Description and 1990s dust climatology*, J. Geophys. Res., 108(D14), 4416*,
2082 doi:10.1029/2002JD002775, 2003.
2083
2084 Zhang, H., Kondragunta, S., Laszlo, I., & Zhou, M. (2020a). Improving GOES Advanced
2085 Baseline Imager (ABI) aerosol optical depth (AOD) retrievals using an empirical bias correction
2086 algorithm. *Atmos. Meas. Tech. 13, 5955–5975*, doi:10.5194/amt-13-5955-2020.
2087
2088 Zhang, J., Spurr, R.J.D., Reid, J.S., Xian, P.,Colarco, P.R., Campbell, J.R., et al. (2020b).
2089 Development of an Ozone Monitoring Instrument (OMI) aerosol index (AI) data assimilation
2090 scheme for aerosol modeling over bright surfaces – a step toward direct radiance assimilation in
2091 the UV spectrum. *Geosci. Model Dev, 14, 27–42*, doi:10.5194/gmd-14-27-2021.
2092
2093 Zhang, J., Campbell, J.R., Reid, J.S., Westphal, D.L., Baker, N.L., Campbell, W.F., & Hyer, E.J.
2094 (2011). Evaluating the impact of assimilating CALIOP-derived aerosol extinction profiles on a
2095 global mass transport model. *Geophys. Res. Lett., 38, L14801*, doi:10.1029/2011GL04773.
2096
2097 Zhu, L., Val Martin, M., Hecobian, A., Deeter, M.N., Gatti, L.V., Kahn, R.A., & Fischer, E.V.
2098 (2018a). Development and implementation of a new biomass burning emissions injection height
2099 scheme for the GEOS-Chem model. *Geosci. Model Develop*. 11, 4103–4116, doi:10.5194/gmd-
2100 11-4103-2018.
2101
2102 Zhu, Y., Rosenfeld, D., & Li, Z. (2018b). Under what conditions can we trust retrieved cloud
2103 drop concentrations in broken marine stratocumulus? *J. Geophys. Res. Atmos. 123, 8754–8767*,
2104 doi:.
2105

Zieger, P., Fierz-Schmidhauser, R., Weingartner, E., & Baltensperger, U. (2013). Effects of relative humidity on aerosol light scattering: results from different European sites. *Atmos. Chem. Phys., 13, 10609–10631*, doi:10.5194/acp-13-10609-2013